國立臺灣大學工學院機械工程學研究所

碩士論文

Department of Mechanical Engineering
College of Engineering
National Taiwan University

Master Thesis

基於能量函數與倒單擺模型之雙足機器人步態軌跡規劃與控制

Walking Pattern Trajectory Planning and Control Based on Energy Function and Inverse Pendulum Model for Biped Robot

張宏毅

Chang, Hong-Yi

指導教授：羅仁權 博士，陽毅平 博士

Advisor: Ren C. Luo, Ph.D., Yee-Pien Yang, Ph.D.

中華民國 100 年 7 月

July 2011

`

致謝

在台大生活了兩年，我的學生生涯終於要劃下句點。一直引頸期盼著這一天的到來，現在真的要離開這個地方，還是難免感到不捨。

二年前從中正大學機械系申請上了台大機械所。當時適逢我現在的指導老師，羅仁權教授，從中正大學校長卸任後轉調台大，於是我強烈的感受到這命運的安排，彷彿命運要再度把離開中正的這兩人再度緊緊的繫在一起，在這種使命感的驅使下，我加入了由羅仁權教授所主持的智慧型機器人與自動化實驗室。

事實上，這果然也是命運的安排，在碩士班的這兩年，老師提供了足夠的經費讓我研究雙足機器人的行走步態，這個題目是我從高中開始就一直想做的，記得當時還很幼稚的拿著自由鋼彈橡皮鑰匙圈去問當時正在攻讀機械所博士班的教官，我:“請問教官，機械系有沒有在做這個阿(手指著鋼彈)”，教官:”當然有阿”，當時聽到教官的回答後我興奮極了，後來才知道原來他說”有”是說機械系有在做橡皮材料鑰匙圈……..

不過不管怎樣，最後我總算有做到我想做的研究，而在這兩年的研究生崖中，首先要感謝我的恩師羅仁權教授。在這兩年的歲月中，他不但提供了充裕的經費和設備讓我有機會親自動手打造雙足機器人，也不時與我討論研究方向及內容。他也是我的人生導師，讓我見識到宏觀的國際視野和台灣人的草根性情是如何並存於一個人身上，以及成就大事業背後所需要的毅力和韌性。

接著要感謝我的共同指導陽毅平教授、蘇國嵐教授願意在百忙之中撥空擔任我的

論文口試委員，您們寶貴的意見使我的論文更臻完美。

這兩年有許多修課經驗也讓我獲益良多。感謝羅仁權教授開授的”機器人感測與控制”，引領我宏觀整個機器人的領域，還有黃漢邦教授、林沛群教授開授的”機器人簡介”，讓我對關節型機器人的軌跡規劃與對這個世界的四個維度(三維空間+時間)的感覺進入另一個層次。

感謝博班學長彭鐿文，在這兩年內給予我許多技術上的指導，讓我了解到控制不再是僅止於數學上的紙上談兵，而是實際對整個控制系統有強烈的實際感覺，另外還有很多具有建設性的意見，助我突破了不少研究上的困境。此外還要感謝博士班的陳金成學長，學弟(同時也是我弟弟)張宏豪，以及實驗室的研發替代役簡安甫，因為有你們的幫忙，整台雙足機器人的硬體才能架的起來。另外在寫程式上，我要特別感謝徐偉隆與林献彰兩位學長，因為有兩位學長的幫忙，才能讓我得以對程式細節的透徹了解。而已經畢業的碩班學長陳敬文、黃千豪、吳士強、林瑜智，一年來承蒙各位對我的照顧，希望你們在仕途上一路順風。

感謝這兩年來與我同甘共苦的八位同窗們：蒲奕豪、黃俊諺、林子達、易春億、張書瑞、高竟中、蔡明傑、黃健桀，以及後來進入實驗室的碩一學弟：張宏豪、陳冠宇、林佩嫻、吳諺彰、施博翰，還有博士班的徐瑋隆學長，實驗室有很多繁瑣的例行工作，在我這一年來擔任大師兄的期間，感謝各位每次的配合，才得以讓實驗室的DEMO 每次都得以成功進行。

感謝盡責的助理施欣宜、張心紜、曾利瑜協助打點行政庶務，讓我們能夠更加專

心於學業和研究工作中。

感謝生我養我的父母，二十多年來一直給我很好的讀書環境，也全力支持我所有的興趣。你們是我的精神依靠，也是我努力完成學業最重要的理由。

感謝老天爺為我的人生安排這些人、這些事、這段特別的旅程。兩年的研究生涯讓我的專業能力更上一層樓；而其間發生的許多酸甜苦辣，如同社會縮影般的實驗室生態，也讓我對人生有了更多的體悟。

張宏毅　謹誌

中華民國一百年七月

中文摘要

在許多雙足機器人研究議題上，為了要控制行走的穩定性，髖部的軌跡通常都會規劃在同一水平面上，因此當這些機器人在行走時膝蓋總是彎曲的。然而，這一點都不像我們人類的行走方式。

為了解決這個問題，我們發展一套能使雙足機器人呈現類人式走法(膝蓋打直)且能穩定行走的步態軌跡生成演算法。首先，本研究先利用 SOLIDWORKS 先建立一個雙足機器人的 3D 模型，接著將其匯入 Matlab 軟體的 Simmechanics 的重力場環境中，接著藉由本演算法寫成的軌跡產生器來生成步態，並調整其中的兩個本演算法提出的穩定參數， 直到模擬環境中的雙足機器人能行走。最後，再將他們套用於實際雙足機器人的軌跡產生器來產生軌跡。然而，實體的雙足機器人與模擬環境中的數學模型不盡相同。因此這兩個穩定參數雖已在模擬環境中精練過，但仍需就實體雙足機器人行走的姿勢(前傾或後倒)來進行些微調整，這部分可藉由高速攝影機來擷取行走時的情況，並依照本論文提出之方法做些微調整，最後即可讓實體雙足機器人行走。

從本論文最後的模擬與實驗可證明，建立在我們提出演算法上的軌跡產生器確實能夠產生各種大小步伐和不同行走時間的穩定步態，且這些步態與世界上大部分雙足機器人(如 ASIMO, HRP 系列)彎著膝蓋行走的走法不同，是為直立行走的步態。

此外，從本論文的截圖與其說明中，可清楚看出各張截圖在本演算法中所代表的各個時態與含義，每張截圖皆為本理論的時間軸中的各個時間點，在這些不同的時

間點中，我們可看到其對應分解動作，與人類行走方式確實有著極大的相似。

ABSTRACT

In many research of biped robotics, for controlling the walking stability of the robot, the hip trajectory is planned at the same height, so the knees of the robot would bend while walking. However, this does not make sense when humans walk.

To deal with the problem, in this thesis, we develop a walking pattern generating algorithm, which would enable the biped robot walking like human (stretch knee walking). First of all, we build a 3D biped robot model by using SOLIDWORKS, and then convert it into gravitational simulation of Simmechanics of Malab software. We generate its walking pattern by the trajectory generator based on the algorithm of this research, and tune its two parameters of stability until the robot in simulation can walk. Finally, we apply the two parameters to the trajectory generator of the actual biped robot to generate the stable pattern. However, there exist modeling errors between the actual biped robot and the model in simulation. Therefore, although we have refined the two parameters in simulation, they still have to be adjusted slightly according to actual walking postures (fall down forward or backward). For this reason, we can use high speed camera to get the actual walking information, and tune the parameters slightly according to the methods in the thesis. Finally, we would enable the robot to walk.

From our simulation and experiment, the trajectory generator based on our algorithm indeed can generate several stable patterns with different step length and step time, and

these knee-stretching patterns are different from the most biped robots in the world (such as ASIMO and HRP series), which walk with knee-bending patterns.

Furthermore, from the snapshots and their illustrations, we can understand the process and meaning in each snapshot. Each snapshot represents a moment of the time axis in our algorithm, and we can see there are many similar points with the human walking behavior from the corresponding separated behavior in each snapshot.

Table of Content

List of Figures

List of Tables

`

Chapter 1 INTRDOCTION

1.1 Motivation

In recent years, many countries such as Japan, Korea and USA, have developed a lot of human size biped robots. These robots have human-like upper and lower limbs, and they are already used in many fields, such as entertainment, home care and military. However, although they can mimic many behaviors of humans, they could not perform naturally like humans, especially on walking. In [1] , for controlling the walking stability of the robot, the hip trajectory is planned at the same height, so the knees of the robot would bend while walking. However, this does not make sense when humans walk.

To deal with the problem, in this thesis, we propose a walking algorithm in which we can preserve the walking stability of the robot with stretching its knee, to generate the hip trajectory with different heights.

1.2 Literature Review

1.2.1 ASIMO

ASIMO was created at Honda's Research & Development Wako Fundamental Technical Research Center in Japan. It is the current model in a line of twelve that began in 1986 with E0 (Fig. 1).

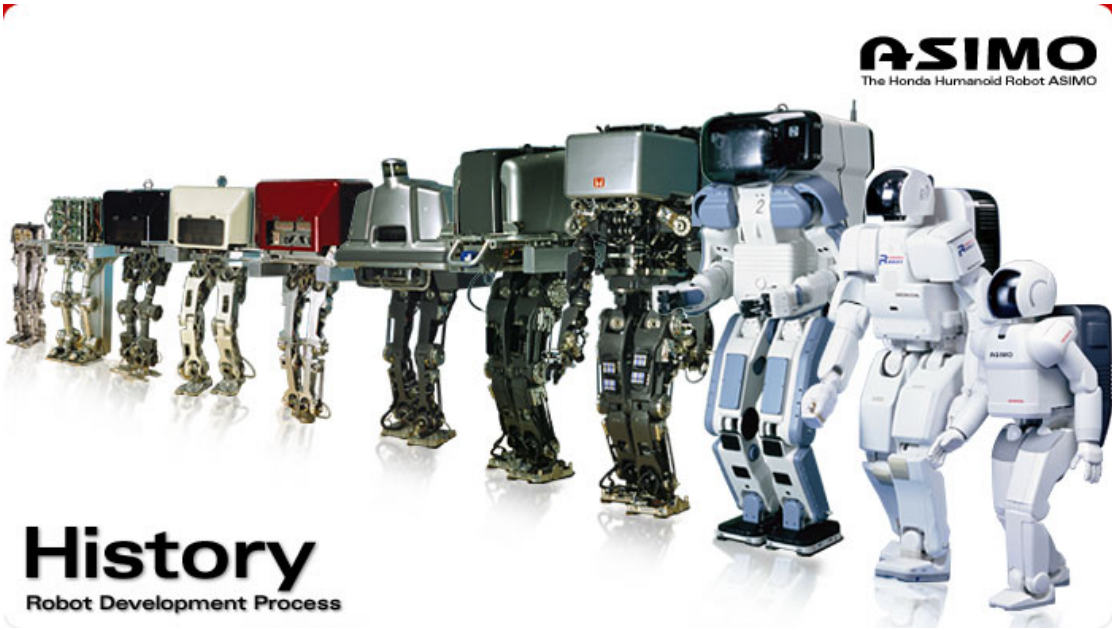

Fig. 1 History of Honda's humanoid robot

ASIMO resembles a child in size and is the most human-like robot HONDA has made so far. The robot has 7 DOF (Degrees of freedom) in each arm — two joints of 3 DOF, shoulder and wrist, giving "Six degrees of freedom" and 1 DOF at the elbow; 6 DOF in each leg — 3 DOF at the crotch, 2 DOF at the ankle and 1 DOF at the knee; and 3 DOF in the neck joint. The hands have 2 DOF — 1 DOF in each thumb and 1 in each finger. This gives a total of 34 DOF in all joints.

Officially, the name is an acronym for "Advanced Step in Innovative MObility" (Fig. 2). Honda's official statements indicate that the robot's name is not refer to science fiction writer and inventor of the Three Laws of Robotics, Isaac Asimov. In Japanese, the name is pronounced ASIMO and, not coincidentally, means "legs also".

Fig. 2 ASIMO

As development continues on ASIMO, today Honda demonstrates ASIMO around the world to encourage and inspire young students to study the sciences. And in the future, ASIMO may serve as another set of eyes, ears, hands and legs for all kinds of people in need. Someday ASIMO might help with important tasks like assisting the elderly or a person confined to a bed or a wheelchair. ASIMO might also perform certain tasks that are dangerous to humans, such as fighting fires or cleaning up toxic spills

1.2.2 WASEDA Series

The other famous institute of studying biped robot in Japan is Humanoid Robotics Institute in Waseda University. People in the institute developed a lot of robot since the starting of WABOT Project in 1970, Fig. 3 shows the roadmap of robot development of WASEDA, while shows the history of the biped robot in Waseda University.

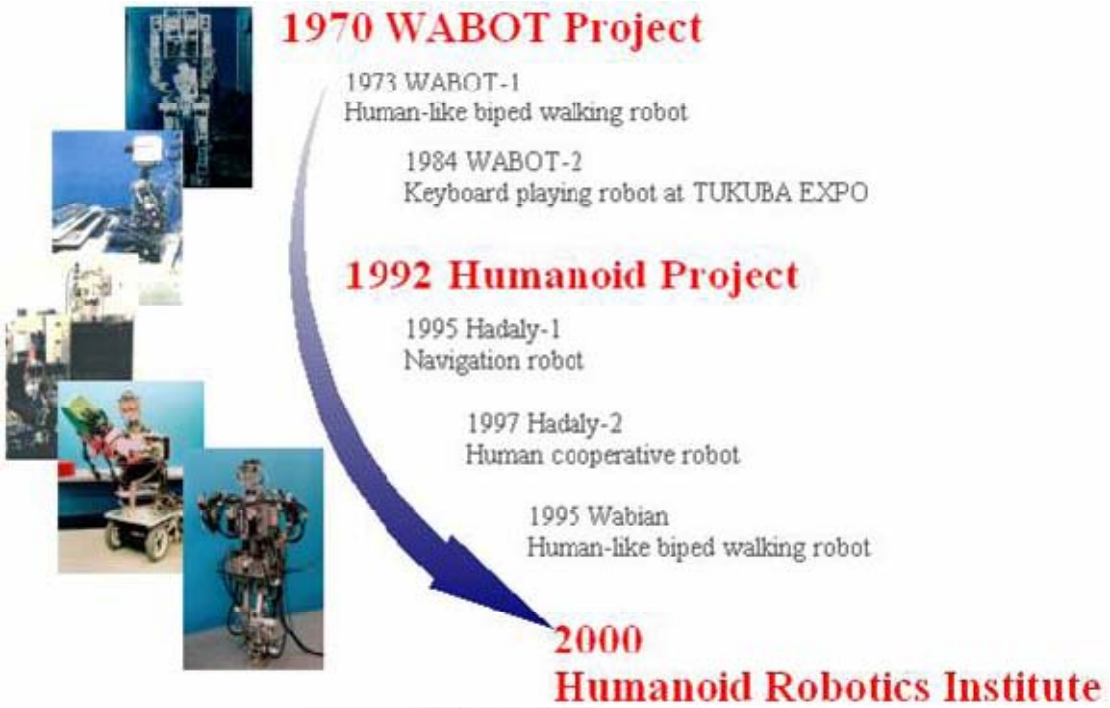

Fig. 3 Roadmap of robot development of WASEDA

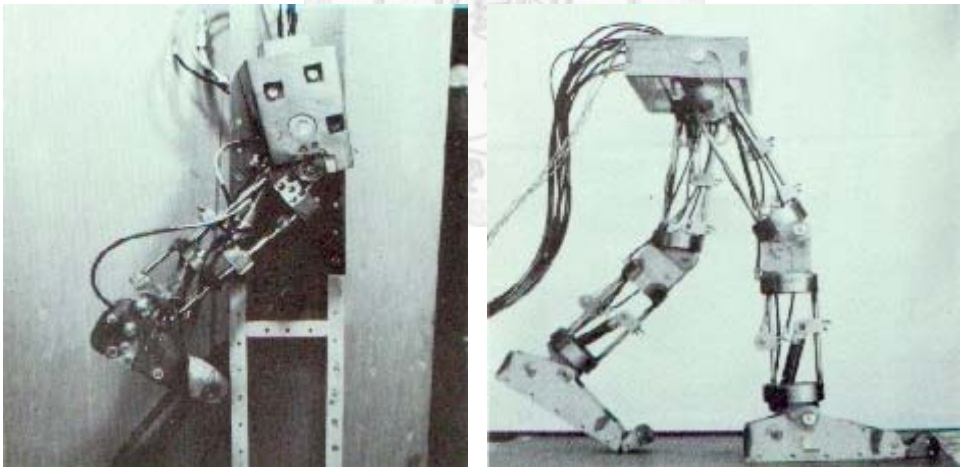

(a)WL-1 (b)WL-3

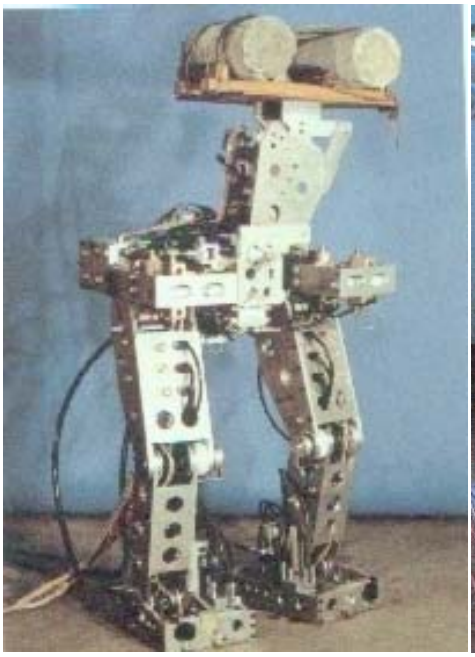

(c)WL-5

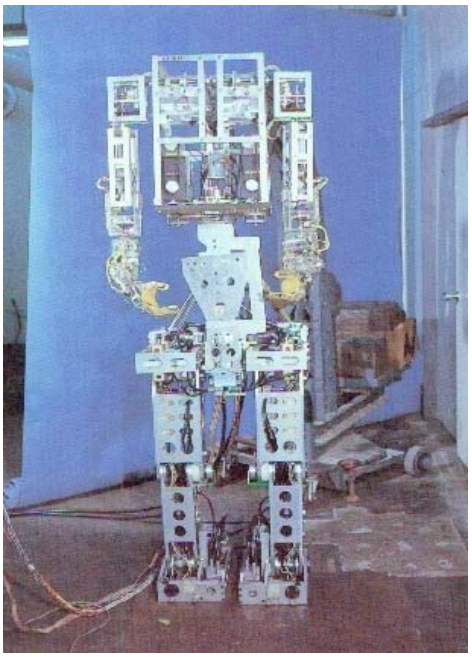

(d)WABOT-1

(e) WL-9DR

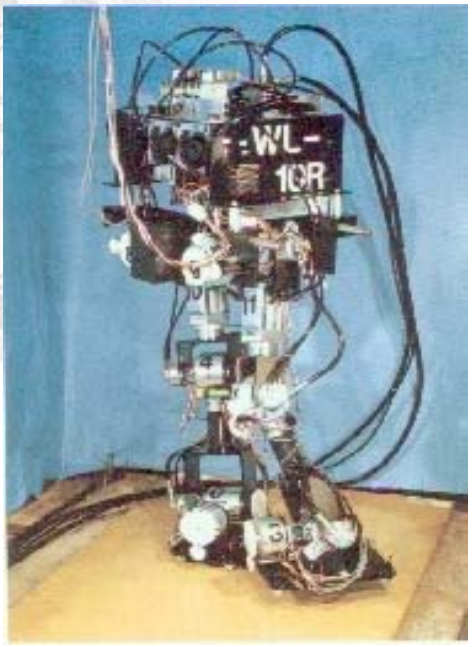

(f) WL-10R

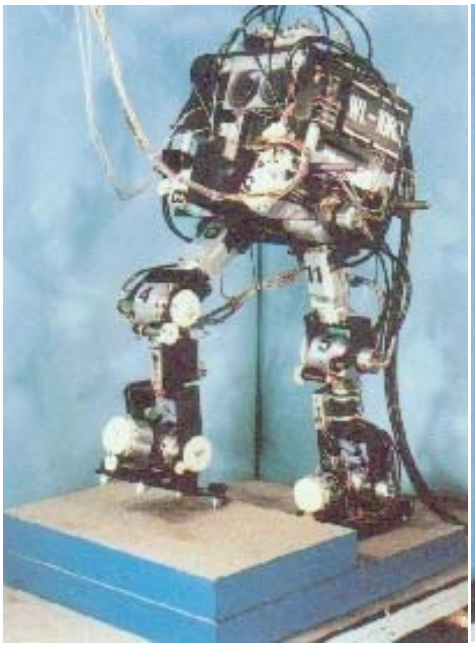

(g) WL-10RD

(h) WL-12

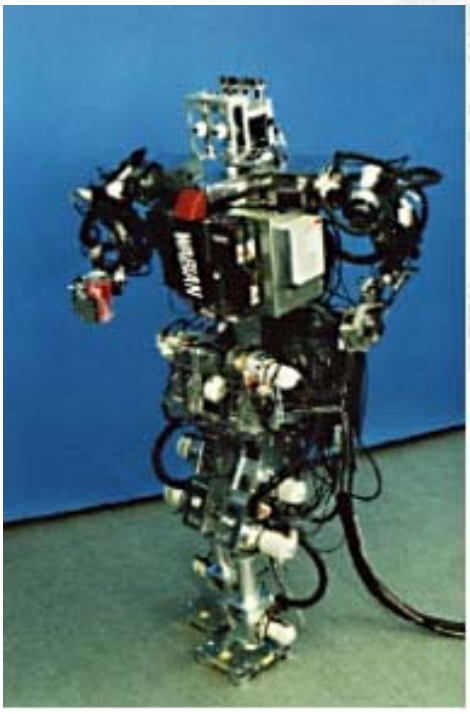

(i) WABIAN

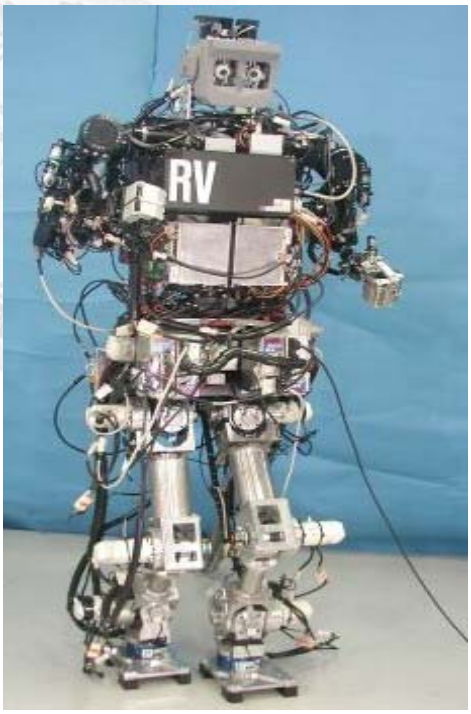

(j) WABIAN-RV

Fig. 4 The history of biped robot in Waseda University.

Now, the newest robot in Waseda University is WABIAN-2R (Fig. 5).

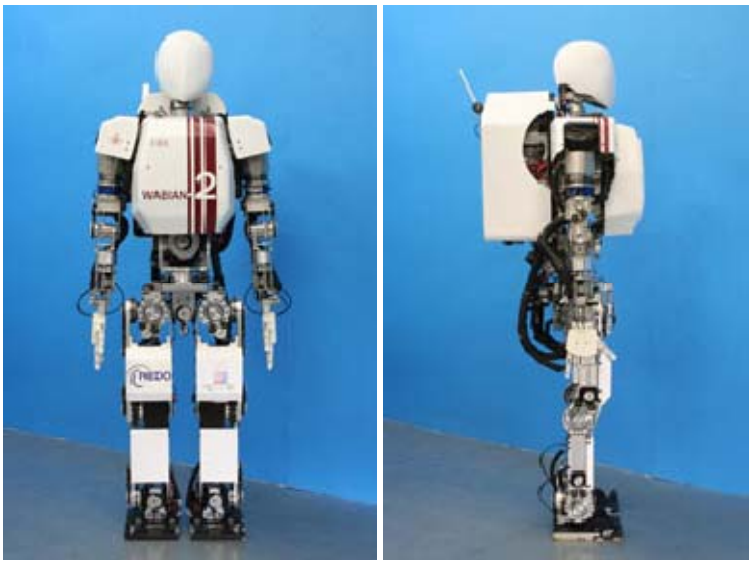

Fig. 5 WABIAN-2R

WABIAN-2 has been designed accordingly in order to develop a humanoid robot with the height of 1475 mm, and the weight of 67.5 kg. This robot was developed In order to mimic the various motions which the human does usually. It consisted of 41-DOFs. (7-DOFs Legs, 2-DOFs Waist, 2-DOFs Trunk, 7-DOF Arms, 3-DOF Hands, and 3-DOF Neck) Link length and movable range are designed in reference of human motion measurement in rehabilitation.

The unique feature of WABIAN-2R is the waist mechanism. Conventional biped humanoid robot has 12 -DOF in the lower limb, and each leg has 6-DOF. Fig. 6 shows DOF configuration of conventional humanoid robot. This is different from humans who have more DOF in the lower limb, and therefore have the ability to realize various walking motions.

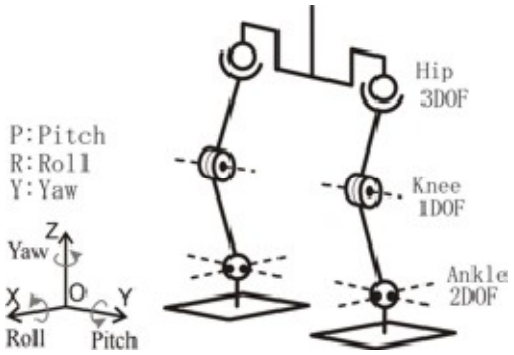

Fig. 6 DOF configuration of conventional humanoid robot

Therefore, in order to realize more human-like walking motions, 2-DOF mechanism (Roll, Yaw) is added to waist part (Fig. 7). This new mechanism has an advantage which makes this robot easier to walk with stretching knee due to the independent orientation of trunk movement.

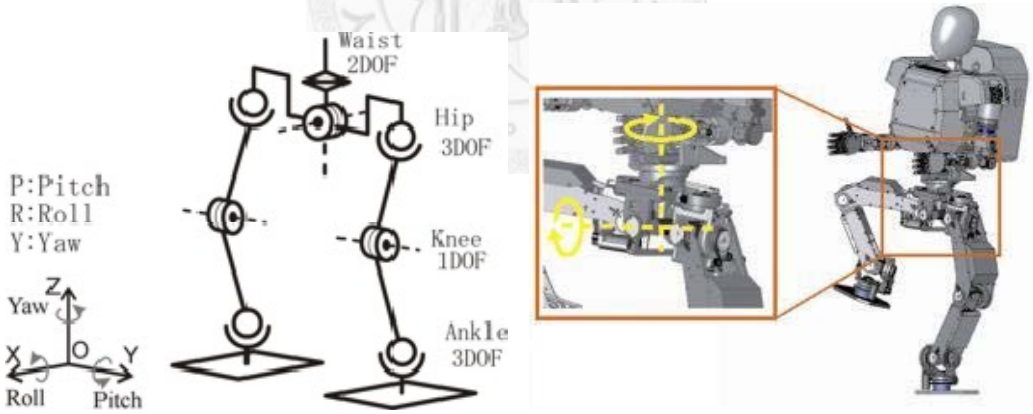

Fig. 7 DOF Configuration of WABIAN-2

1.2.3 PETMAN

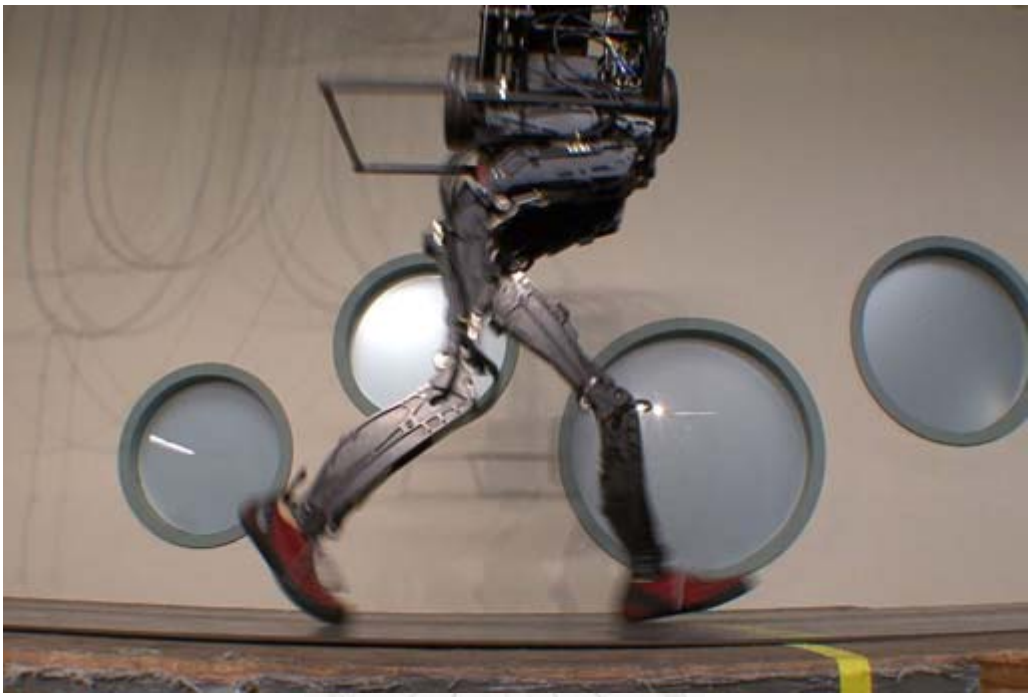

Fig. 8 PETMAN

PETMAN[5] is an anthropomorphic robot made by Boston Dynamics for testing chemical protection clothing used by the US Army. Unlike previous suit testers, which had to be supported mechanically and had a limited repertoire of motion, PETMAN will balance itself and move freely, such as walking, crawling and doing a variety of suit-stressing calisthenics during exposure to chemical warfare agents.

PETMAN will also simulate human physiology within the protective suit by controlling temperature, humidity and sweating when necessary, all to provide realistic test conditions.

Natural, agile movement is essential for PETMAN to simulate how a soldier stresses protective clothing under realistic conditions. The robot will have the shape and size of a standard human, making it the first anthropomorphic robot that moves dynamically like a real person.

1.2.4 Zero Moment Point

Z.M.P(Zero Moment Point) is a concept related with dynamics and control of legged locomotion. This concept was introduced in January 1968 by Miomir Vukobratović and Davor Juričić at The Third All-Union Congress of Theoretical and Applied Mechanics in Moscow.

From that time, many biped robot based on ZMP concept were developed, and this concept was spread widely in the field of biped robot.

As shown in Fig. 9, assume that the ground distributive force can be regarded as an equivalent force N , which is acted on the pressure center p , with a moment M .

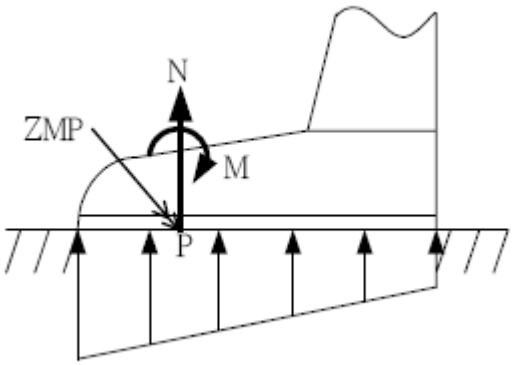

Fig. 9 The ground reactive force of foot

However, in general, the ground could not provide the moment M for the foot. That is, M needs to be zero. Therefore, if the loading on the foot changes, M could not change to a proper value to balance the foot. So the equivalent force N would move to specific a position to compensate M automatically. Therefore, this position would call Zero Moment Point (ZMP).

1.3 Thesis Organization

This thesis is organized as follows. In **Chapter 1**, we present the motivation, objective, and literature review. In **Chapter 2**, we introduce our hardware and software structure of the biped robot, which including sensors, actuator, software and coordinate systems. In **Chapter 3**, we make an analysis of the stability of the robot. In the walking cycle, we divided it in to three processes, which are lowering down, rising up and inverse pendulum process. Lowering down and rising up processes would be combined as "lowering down-rising up process" to analyze its stability. In **Chapter 4**, we would show the simulation result and walking result. Finally, conclusion and main contributions would be shown in **Chapter 5**. The **Chapter 6** is the future works, which describes the problems of the actual biped robot of our experiment we encounter but haven't solved, and some viewpoints and methods for people who continue to study the research to refer.

Chapter 2 SYSTEM STRUCTURE OF BIPED ROBOT

2.1 Hardware Structure

Fig. 10 and Fig. 11 show the 3D CAD model and the actual biped robot, which has 6 degrees of freedom in each leg, and it is 87.6 cm of its height (without trunk), 40 kg of its weight (without batteries). The reduction gear of each joint is composed of a harmonic drive and belt pulley, Table. 1 shows the detail of the reduction ratio and range of each joint. To drive these joints, Maxon motors “EC-4Pole 30, 200 watt with MR encoder 500 cpt” and controllers “EPOS2 50/5” were used as the actuating system of the robot.

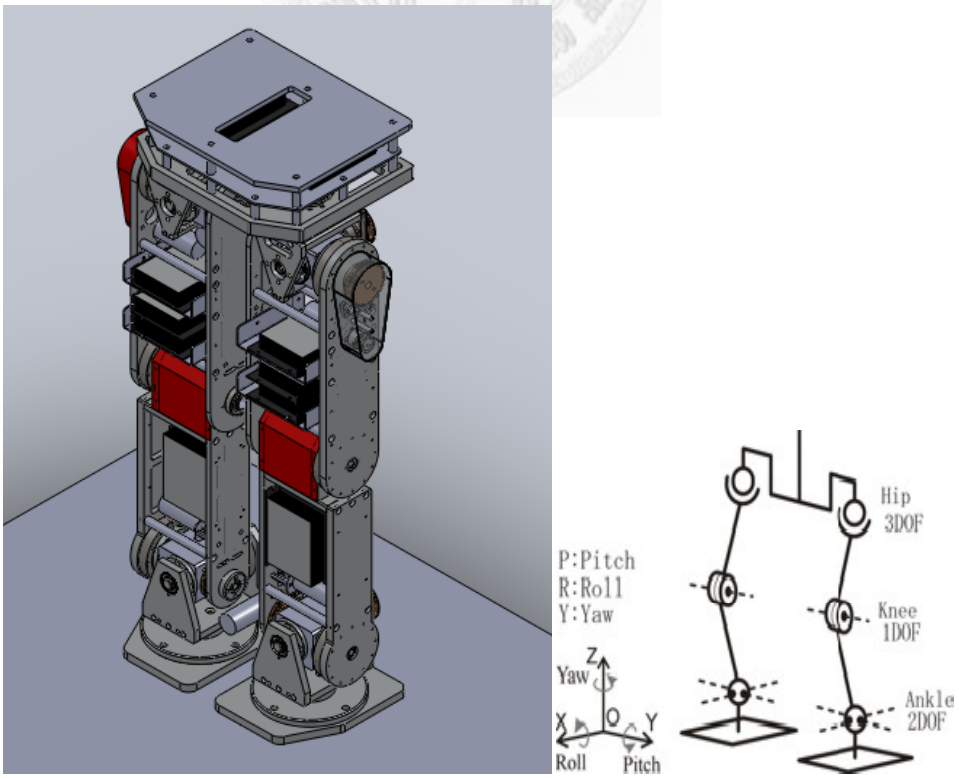

Fig. 10 The 3D CAD model of the biped robot

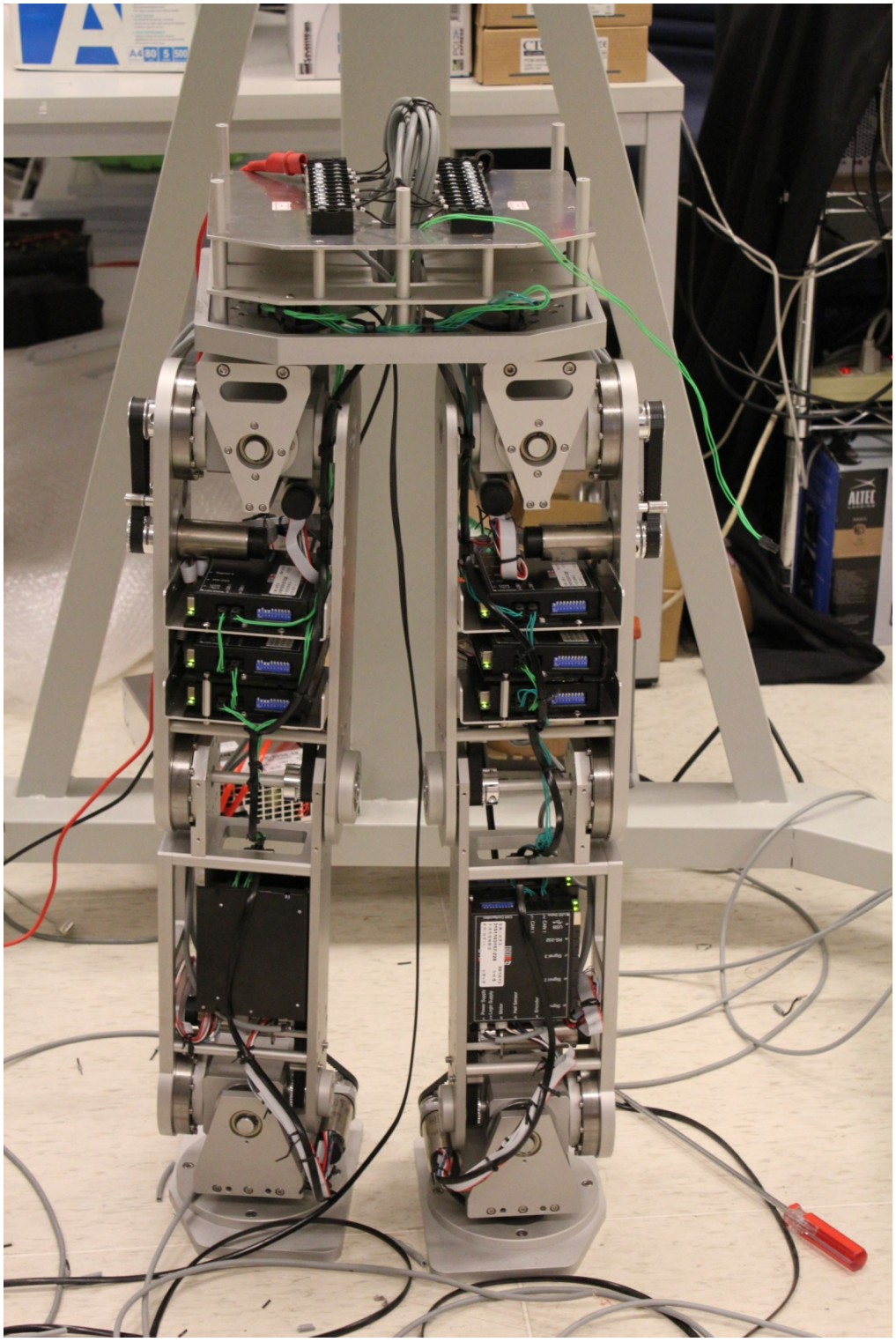

Fig. 11 The actual biped robot

Table. 1 Reduction ratio and range of each joint

	Harmonic Drive	Belt Pulley	Total	Range(degree)
Hip_Yaw	1:100	1:1	1:100	-45~+45
Hip_Roll	1:100	1:3	1:300	-13~+13
Hip_Pitch	1:160	1:1	1:160	-45~+50
Knee	1:160	1:1	1:160	0~+70
Foot_Pitch	1:160	1:1	1:160	-30~+20
Foot_Roll	1:160	1:1.5	1:240	-20~+20

Fig. 12 The Maxon motor and controller

To make communication between the main computer mounted on the robot and

each motor, CANOpen is used here. CANOpen is a high speed communication protocol, which is very popular in modern industry. As shown in Fig. 13, we have to connect first and final driver with 120 omega resistor, since the master of the CANOpen has to know the terminals. The I/O ports of the CANOpen mater is shown in Fig. 14. We just connect the CAN_H, CAN_L, and ground to the first driver. Console can use USB surface to connect CANOpen master and communicate each driver.

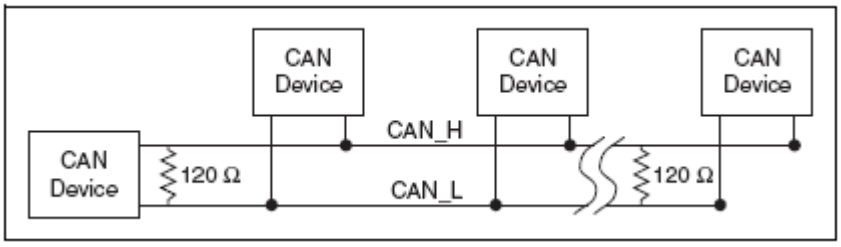

Fig. 13 First and final CAN device have to connect terminal resistances (120 omegas)

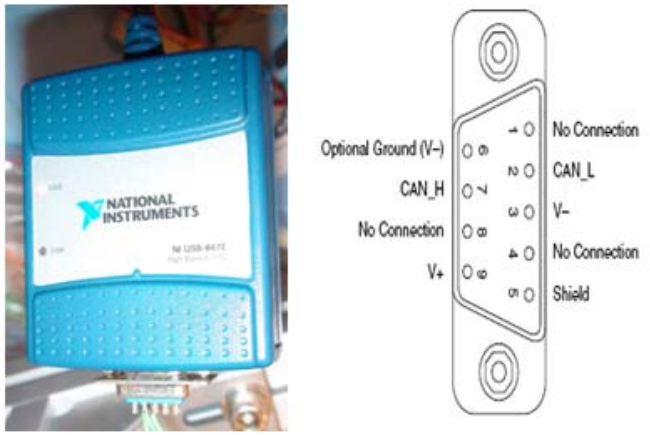

Fig. 14 Master of the CANOpen and the layout of I/O ports

To measure the ground reactive force, the 6-axis force sensor “IFS-67M25T50-

M40BS” is mounted on each foot, which is made by Nitta Corporation. Fig. 15 shows the sensor.

Fig. 15 The 6-axis force sensor “IFS-67M25T50- M40BS”

2.2 Software Structure

To control our biped robot, we use MATLAB and Visual C++ and as our main programs. MATLAB program is used to establish the simulation and compute joint angles, while Visual C++ program is used to establish the human-robot interface, which enables us to control the whole motors of the robot. Fig. 16 shows the structure of using MATLAB and Visual C++.

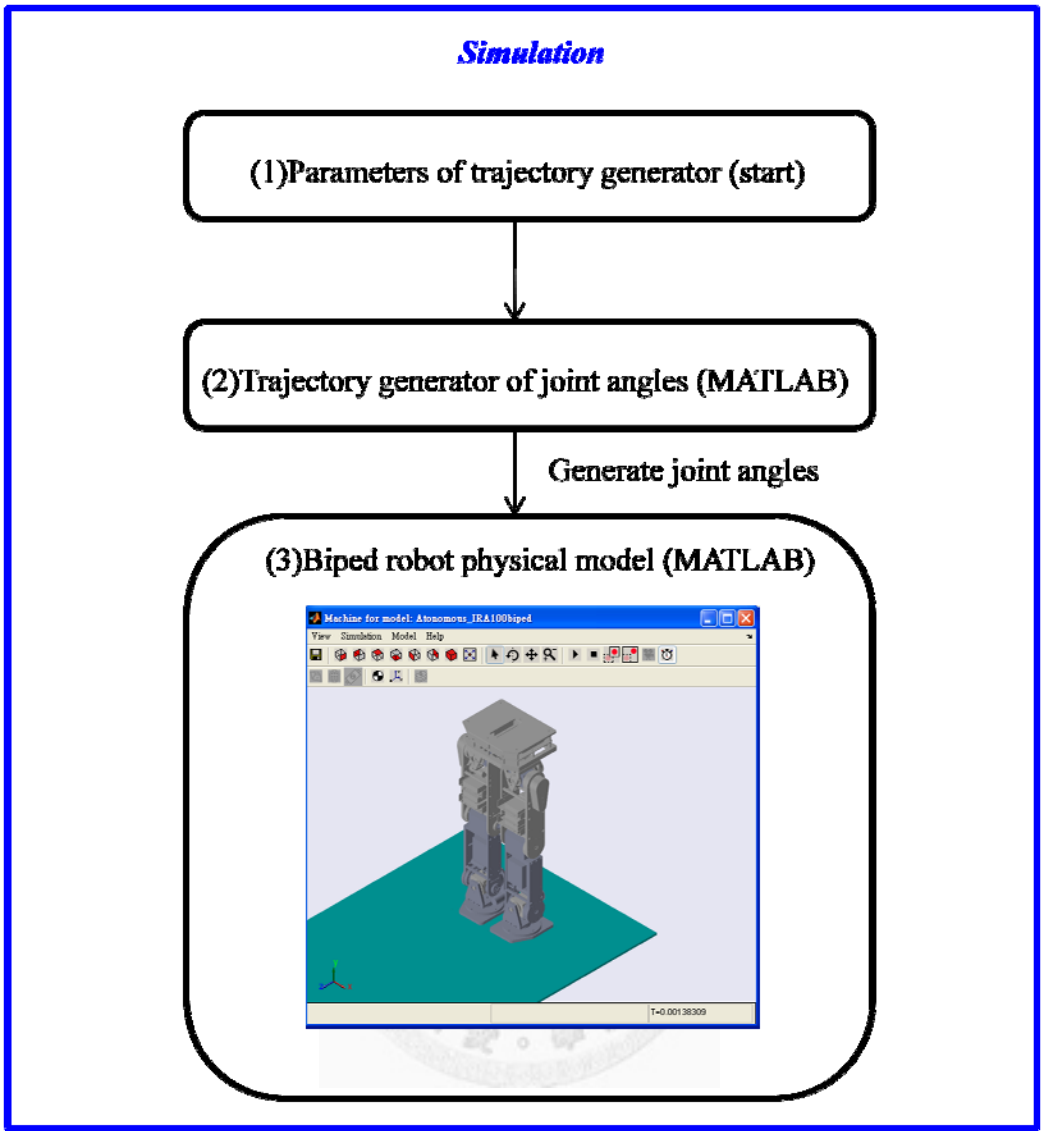
Simulation
(1)Parameters of trajectory generator (start)
(2)Trajectory generator of joint angles (MATLAB)
Generate joint angles
(3)Biped robot physical model (MATLAB)
Machine for model: Atonomous_IRA100biped
View Simulation Model Help
T=0.00138309

(a)

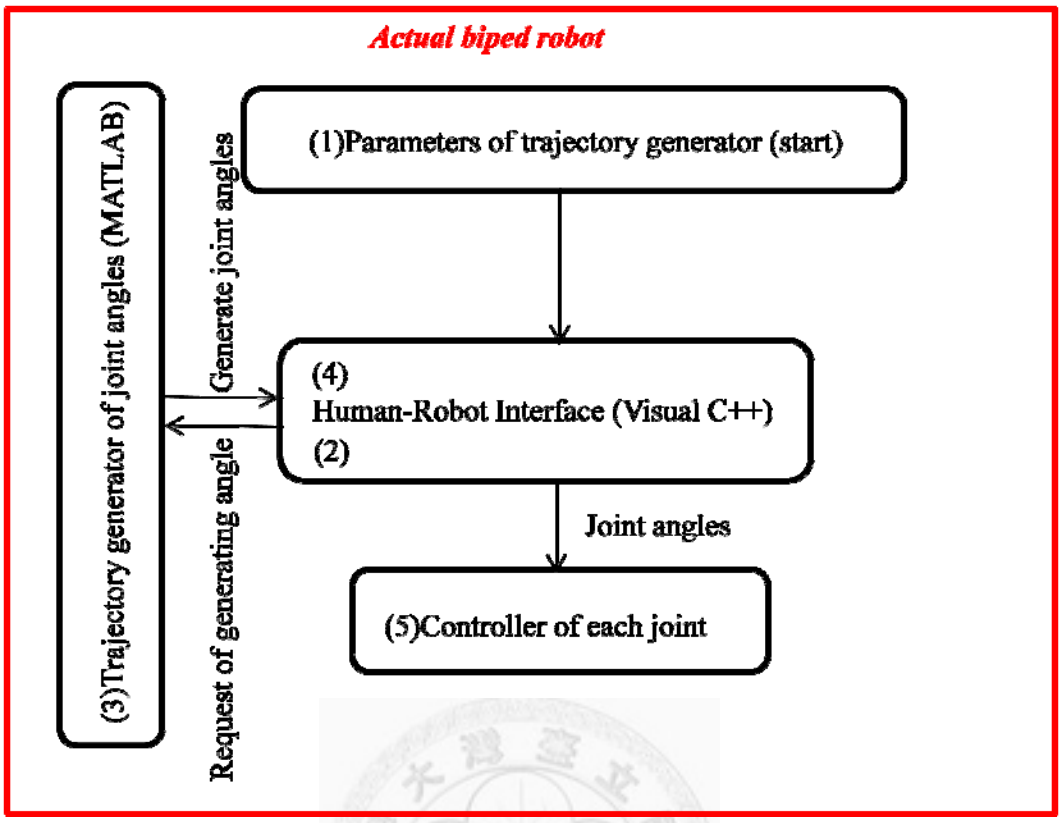

(b)

Fig. 16 The structure of using MATLAB and Visual C++

In general, to communicate sensors and controllers with the main computer for the actual robot depends on Visual C++ program, while MATLAB is used as the computing kernel of the simulation and trajectory generator.

2.3 Robot Coordinate System

In order to determine relationship between posture and each joint of the robot, we need to establish coordinate system. The most popular coordinate system used in robotics is the Denavit-Hartenberg convention. In this convention, each homogeneous transformation that is a 4x4 matrix is represented as a general formula of four basic

transformations. The four basic transformations means the four parameters a_i, α_i, d_i, and θ_i are generally given the names link length, link twist, link offset, and joint angle, respectively. Fig. 17 shows the relationship between two joints in DH coordinate system

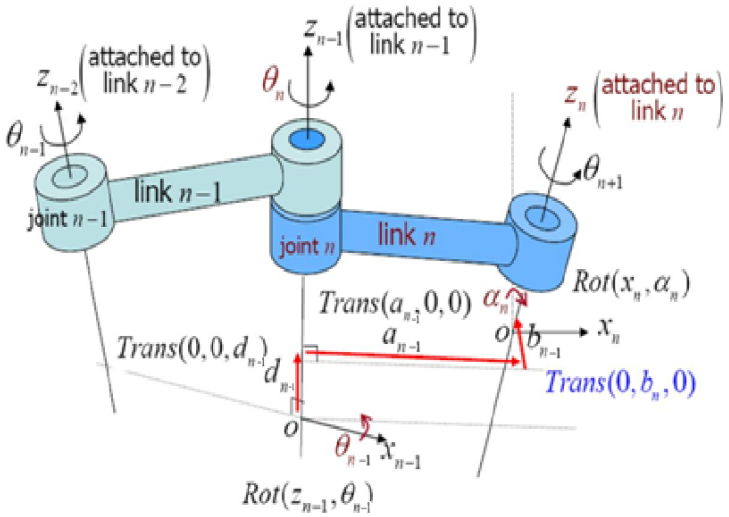

Fig. 17 The relationship between two joints in DH coordinate system

2.3.1 Robot Forward Kinematic Analysis

The D-H convention allows the construction of the forward kinematics function by composing the coordinate transformations into one homogeneous transformation matrix:

$$T_i^{i-1} = \begin{bmatrix} \cos\theta_i & -\sin\theta_i\cos\alpha_i & \sin\theta_i\sin\alpha_i & a_i\cos\theta_i \\ \sin\theta_i & \cos\theta_i\cos\alpha_i & -\cos\theta_i\sin\alpha_i & a_i\sin\theta_i \\ 0 & \sin\alpha_i & \cos\alpha_i & d_i \\ 0 & 0 & 0 & 1 \end{bmatrix} \quad (1) \quad .$$

$$ {}^{0}_{6}T = {}^{0}_{1}T\,{}^{1}_{2}T\,{}^{2}_{3}T\,{}^{3}_{4}T\,{}^{4}_{5}T\,{}^{5}_{6}T = \begin{bmatrix} {}^{0}R_6 & {}^{0}P_6 \\ 0 & 1 \end{bmatrix} \qquad (2) \quad . $$

where ${}^{0}P_6$ is 3 × 1 transformation vector, ${}^{0}R_6$ is 3 × 3 rotation matrix, and 0 is 1 × 3 zero vector.

We will get the relationship between the end-effector and the base coordinate from Eq.(2). We may summarize the above procedure based on the D-H convention in the following algorithm for deriving the forward kinematics for any joint robot.

Step l: Locate and label the joint axes z_0….. z_{n-1}.

Step 2: Establish the base frame. Set the origin anywhere on the z_0-axis. The x_0 and y_0 axes are chosen conveniently to form a right-hand frame. For i = 1…..n-1, perform Steps 3 to 5.

Step 3: Locate the origin O_i where the common normal to z_i and z_{i-1} intersects z_i. If z_i intersects z_{i-1} locate O_i at this intersection. If z_i and z_{i-1} are parallel, locate O_i in any convenient position along z_i.

Step 4: Establish x_i along the common normal between z_{i-1} and z_i through O_i, or in the direction normal to the z_{i-1}–$z_i$plane if z_{i-1} and z_i intersect.

Step 5: Establish y_i to complete a right-hand frame.

Step 6: Establish the end-effector frame $o_n x_n y_n z_n$. Assuming the n-th joint is revolute, set z_n = a along the direction z_{n-1}. Establish the origin on conveniently along z_n, preferably at the center of the gripper or at the tip of any tool that the

manipulator may be carrying. Set y_n = s in the direction of the gripper closure and set x_n = n as s × a. If the tool is not a simple gripper set x_n and y_n conveniently to form a right-hand frame.

Step 7: Create a table of link parameters a_i, d_i, α_i, θ_i.

a_{i-1} = distance along x_i from O_i to the intersection of the z_i and z_{i-1} axes.

d_{i-1} = distance along z_{n-1} from O_{i-1} to the intersection of the x_i and x_{i-1} axes. d_{i-1} is variable if joint i is prismatic.

α_{i-1} = the angle between z_{n-1} and z_i measured about x_i.

θ_{i-1} = the angle between x_{i-1} and xi measured about z_{n-1}. θ_i is variable if joint i is revolute.

Step 8: Form the homogeneous transformation matrices T_i by substituting the above parameters into Eq. (1).

Step 9: Form $T_{0n} = T_1 \ldots T_n$. This then gives the position and orientation of the tool frame expressed in base coordinates.

2.3.2 Robot Inverse Kinematic Analysis

The equations we found for solving the inverse kinematic problem of robots can directly be used to drive the robot to a position. In fact, no robot would actually use the forward kinematic equations to solve for these results. The equations used are the set of six (or fewer, depending on the number of joints) equations enable us to calculate the

joint values. In other words, we must calculate the inverse solution and derive these equations and, in return, use them to drive the robot to position desired.

Equation (3), (4) represent the differential relationship between individual variables and the function. The Jacobian can be calculated by taking the derivative of each equation with respect to all variables.

$$Y_i = f_i(x_1, x_2, x_3, \cdots, x_j) \quad (3) \ .$$

$$\begin{cases} \delta Y_1 = \dfrac{\partial f_1}{\partial x_1}\delta x_1 + \dfrac{\partial f_1}{\partial x_2}\delta x_2 + \cdots + \dfrac{\partial f_1}{\partial x_j}\delta x_j \\ \delta Y_2 = \dfrac{\partial f_2}{\partial x_1}\delta x_1 + \dfrac{\partial f_2}{\partial x_2}\delta x_2 + \cdots + \dfrac{\partial f_2}{\partial x_j}\delta x_j \\ \vdots \\ \delta Y_i = \dfrac{\partial f_i}{\partial x_1}\delta x_1 + \dfrac{\partial f_i}{\partial x_2}\delta x_2 + \cdots + \dfrac{\partial f_i}{\partial x_j}\delta x_j \end{cases} \quad (4) \ .$$

As we are able to express their position differential change in the joint variation space Equation (5).

$$\begin{bmatrix} dx \\ dy \\ dz \\ \delta x \\ \delta y \\ \delta z \end{bmatrix} = \begin{bmatrix} & & \\ Robot & & \\ Jaobian & & \\ & & \\ & & \\ & & \end{bmatrix} \begin{bmatrix} d\theta_1 \\ d\theta_2 \\ d\theta_3 \\ d\theta_4 \\ d\theta_5 \\ d\theta_6 \end{bmatrix} \quad \text{or} \quad [D] = [J][D_\theta] \quad (5) \ .$$

Where dx, dy, and dz in [D] represent the differential motion of the hand along the x-axis, y-axis, and z-axis, respectively, δx, δy, and δz in [D] represent the differential

rotations of the hand around the x-axis, y-axis, z-axis, respectively, and represents the differential motions of the joints. We can divide the differential motion into differential transformations (translations and rotations).

- Differential translations

  The frame has moved a differential amount along the three axes. The differential translations can be represented by Trans (dx, dy, dz).

- Differential rotations

  A differential rotation is a small rotation of the frame. It is generally represented by Rot(k, θ).

- Differential transformations (translations and rotations)

$$\sin \delta x = \delta x \quad (6)$$

$$\cos \delta x = 1 \text{ (in radians)}$$

Because the rotation is small, the rotation matrix can be represented:

$$Rot(x, \delta x) = \begin{bmatrix} 1 & 0 & 0 & 0 \\ 0 & 1 & -\delta x & 0 \\ 0 & \delta x & 1 & 0 \\ 0 & 0 & 0 & 1 \end{bmatrix} \quad (7)$$

Thus, we assume differential motion with axis k, it is combine with x axis, y axis and z axis differential motions Equation (5).

$$Rot(k,d\theta) = Rot(x,\delta x)Rot(y,\delta y)Rot(z,\delta z) \tag{8}$$

$$= \begin{bmatrix} 1 & 0 & 0 & 0 \\ 0 & 1 & -\delta x & 0 \\ 0 & \delta x & 1 & 0 \\ 0 & 0 & 0 & 1 \end{bmatrix} \begin{bmatrix} 1 & 0 & \delta y & 0 \\ 0 & 1 & 0 & 0 \\ -\delta y & 0 & 1 & 0 \\ 0 & 0 & 0 & 1 \end{bmatrix} \begin{bmatrix} 1 & -\delta z & 0 & 0 \\ \delta z & 1 & 0 & 0 \\ 0 & 0 & 1 & 0 \\ 0 & 0 & 0 & 1 \end{bmatrix}$$

$$= \begin{bmatrix} 1 & -\delta z & \delta y & 0 \\ \delta x\delta y + \delta z & -\delta x\delta y\delta z + 1 & -\delta x & 0 \\ -\delta y + \delta x\delta z & \delta x + \delta y\delta z & 1 & 0 \\ 0 & 0 & 0 & 1 \end{bmatrix}$$

If we neglect all higher order differentials, we get:

$$Rot(k,d\theta) = Rot(x,\delta x)Rot(y,\delta y)Rot(z,\delta z) \tag{9}$$

$$= \begin{bmatrix} 1 & -\delta z & \delta y & 0 \\ \delta x\delta y + \delta z & -\delta x\delta y\delta z + 1 & -\delta x & 0 \\ -\delta y + \delta x\delta z & \delta x + \delta y\delta z & 1 & 0 \\ 0 & 0 & 0 & 1 \end{bmatrix} = \begin{bmatrix} 1 & -\delta z & \delta y & 0 \\ \delta z & 1 & -\delta x & 0 \\ -\delta y & \delta x & 1 & 0 \\ 0 & 0 & 0 & 1 \end{bmatrix}$$

And if we want to get differential operator, we can combine differential translations, differential rotation and subtracting the unit matrix as following:

$$\Delta = Trans(dx,dy,dz) \times Rot(k,d\theta) - I \tag{10}$$

$$= \begin{bmatrix} 1 & 0 & 0 & dx \\ 0 & 1 & 0 & dy \\ 0 & 0 & 1 & dz \\ 0 & 0 & 0 & 1 \end{bmatrix} \begin{bmatrix} 1 & -\delta z & \delta y & 0 \\ \delta z & 1 & -\delta x & 0 \\ -\delta y & \delta x & 1 & 0 \\ 0 & 0 & 0 & 1 \end{bmatrix} - \begin{bmatrix} 1 & 0 & 0 & 0 \\ 0 & 1 & 0 & 0 \\ 0 & 0 & 1 & 0 \\ 0 & 0 & 0 & 1 \end{bmatrix}$$

$$= \begin{bmatrix} 0 & -\delta z & \delta y & dx \\ \delta z & 0 & -\delta x & dy \\ -\delta y & \delta x & 0 & dz \\ 0 & 0 & 0 & 0 \end{bmatrix}$$

The Jacobian of the robot will create the link between the joint movements and the hand movement; we can use the calculation of the Jacobian as follows:

$$[D]=[J][D_\theta] \quad (11)\ .$$

$$[J^{-1}][D]=[J^{-1}][J][D_\theta] \quad (12)\ .$$

$$[D_\theta]=[J^{-1}][D] \quad (13)\ .$$

Finally, the discrete form of the general solution provided by inverse kinematics is:

$$\Delta\theta = J^{+}\Delta x + (I - J^{+}J)\Delta z \quad (14)\ .$$

Where$\Delta\theta$ is the unknown vector in the joint variation space, Δx is variation of one or more end effectors position and orientation in Cartesian space, J^{+} is the unique pseudo-inverse of J providing the minimum norm solution, and Δz describes a secondary behavior in the joint variation space.

2.3.3 Trajectory Generator

To establish the trajectory generator, we use the Robotics Toolbox in MATLAB, which is a powerful toolbox that can help us to compute the kinematics of multi- D.O.F. system as long as we construct the D.H. coordinate system of the robot for it.

Here, we construct two D.H. coordinate systems of the robot. One is for the front leg, while the other is for the rear leg, respectively. Table. 2 and Table. 3 show the D.H. coordinate systems of the robot.

Table. 2 D.H. coordinate system of front leg

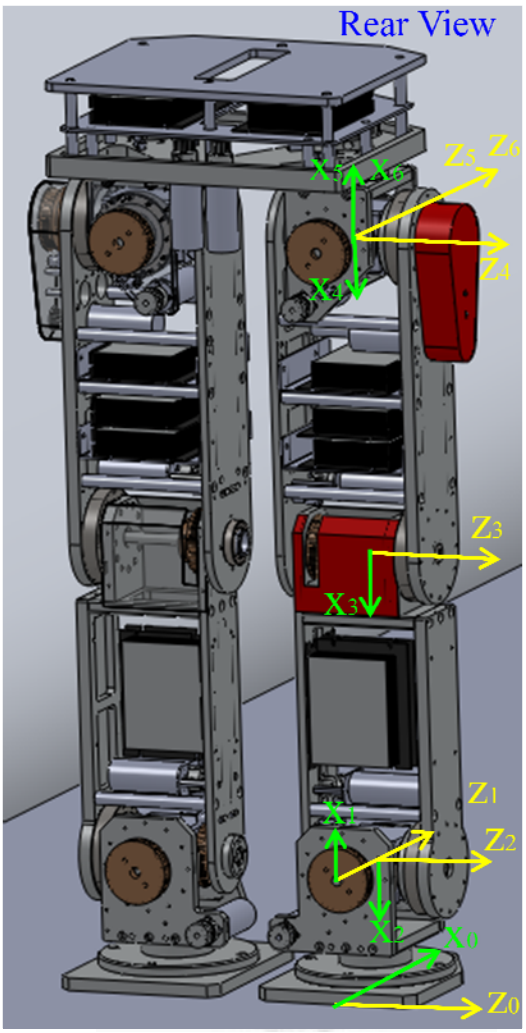

	α (rad)	a (cm)	θ (rad)	d (cm)	θ_{init} (rad)
1	$\frac{\pi}{2}$	11.5	θ_1	0	$\frac{\pi}{2}$
2	$\frac{\pi}{2}$	0	θ_2	10	π
3	0	-30	θ_3	0	0
4	0	-30	θ_4	0	0
5	$\frac{\pi}{2}$	0	θ_5	0	π
6	0	0	θ_6	0	0

Table. 3 D.H. coordinate system of rear leg

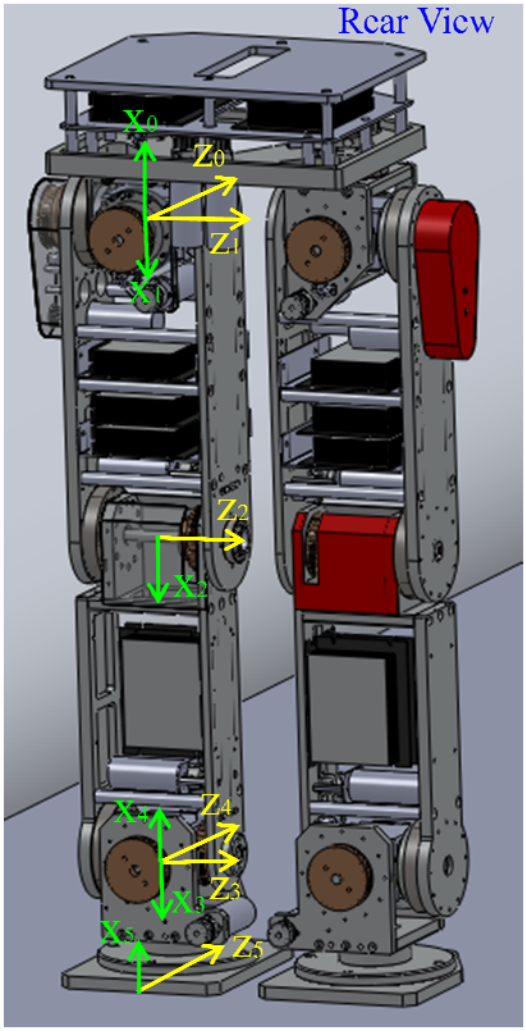

	α (rad)	a (cm)	θ (rad)	d (cm)	θ_{init} (rad)
1	$\frac{\pi}{2}$	0	θ_1	0	π
2	0	30	θ_2	0	0
3	0	30	θ_3	0	0
4	$\frac{\pi}{2}$	0	θ_4	0	π
5	0	-11.5	θ_5	-10	0

To generate joint trajectory, we have to establish the trajectory generator. Therefore, we use the following steps to establish it:

1. Plan the hip trajectory at pitch direction based on our algorithm in **Chapter 3** in 2D Cartesian (planar) space.
2. Use the geometric method to solve planar inverse kinematics to get the pitch joints of the front leg.
3. Plane Roll joints of the front leg.
4. Use joint angles of the front leg with its D.H. coordinate (Table. 2) to calculate forward kinematics to get actual position vector of hip trajectory in 3D cartesian space.
5. Plane position vector of the foot trajectory of rear leg in 3D cartesian space.
6. Subtract **the position vector of hip trajectory** from **the Planed position vector of the foot trajectory of rear leg** to get the position vector relative to hip.
7. Solve inverse kinematics with the D.H. coordinate of rear leg (Table. 3) to get each joint angle of rear leg.

Following the above steps, we can generate all joint angles of the robot, and then feed them to each joint controller through CANOpen to realize stable walking. Fig. 18 shows the control structure of the biped robot.

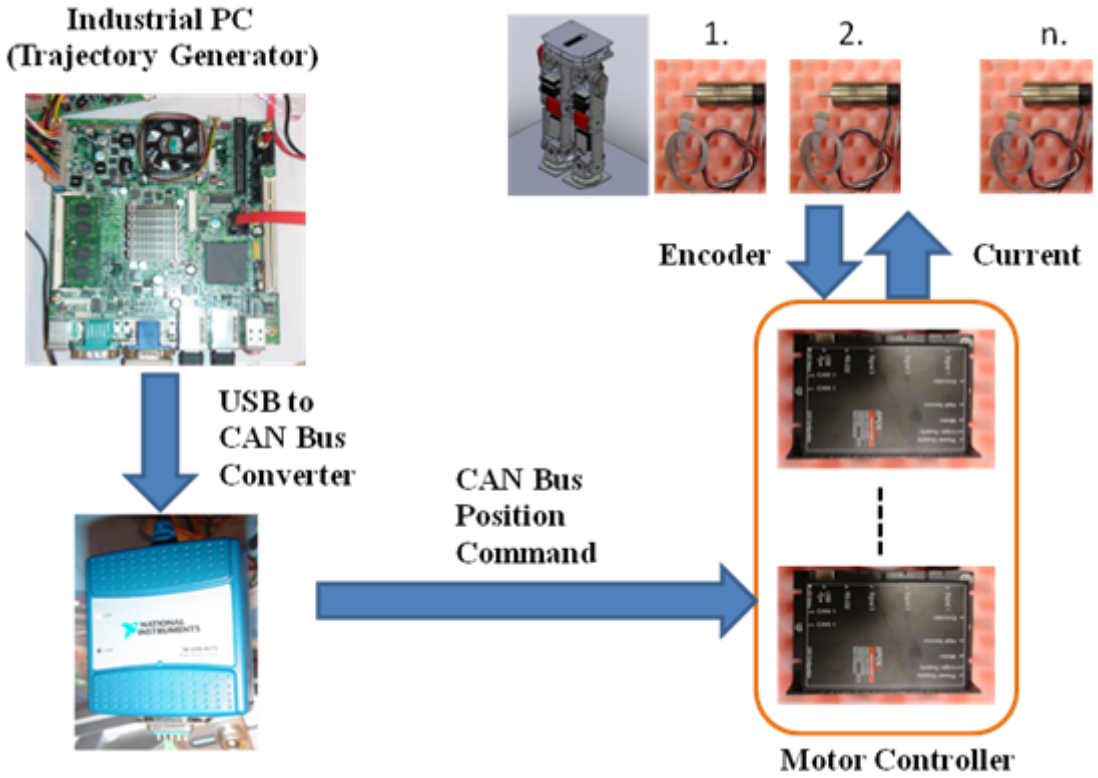

Fig. 18 Control structure of the biped robot.

Chapter 3 WALKING STABILITY ANALYSIS

3.1 Walking Cycle

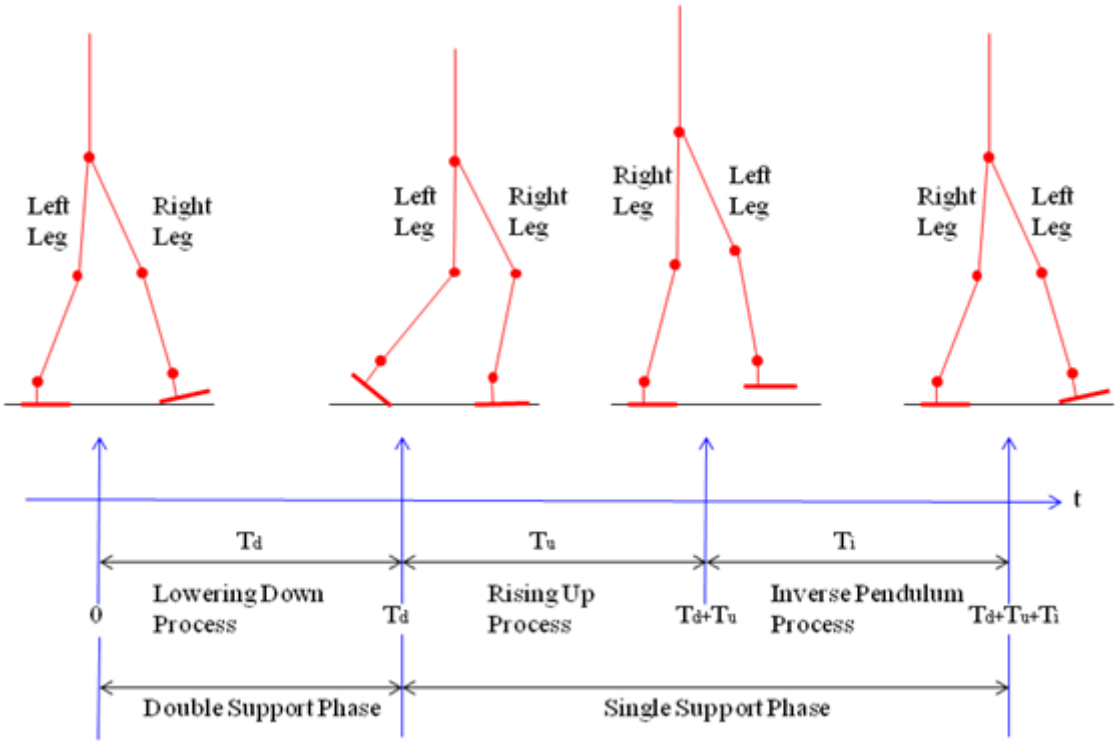

Fig. 19 Walking cycle for one step

In general, biped walking is a periodic cycle, and it always consists of two phases: the double support phase and the single support phase. Here, we divide the walking behavior into three processes: the lowering down process, the rising up process and the inverse pendulum process, respectively. The lowering down process occurs in double support phase while the rising up process and the inverse pendulum process happen in single support phase. Fig. 19 shows the relationship between walking phases and

processes of walking behavior.

As we can see in Fig. 19, the lowering down process occurs during $t = 0 \sim T_d$. In the process, the front leg and the rear leg will cooperate to finish the lower down motion. When time reaches to T_d, the lowering down process will end while rising up process will start. In rising up process, the front leg will stretch to raise the robot while the rear leg will rise and swing from back to front. Then when time reaches to $T_d + T_u$, the walking behavior would enter the inverse pendulum process. In this process, the knee joint of supporting leg will be locked, and the ankle joint would swing the robot forward to prevent it fall down forward. When time reaches to $T_d + T_u + T_i$, the swing leg will touch the ground, and the total posture will be finished. Therefore, one walking cycle would be finished, and then next cycle will be started.

In the following topics, we will focus on the stability of these walking processes. The lowering down and rising up processes would be combined into "lowering down-rising up process", and then discussed in **Chapter 3.2**, while "inverse pendulum process" will be analyzed in **Chapter 3.3**. We would use different degrees to analyze the two processes. That is, different models would be used in different processes.

The main propose in "lowering down-rising up process" is to prevent the robot fall down backward since its COG (center of gravity) is close to the rear edge of the supporting leg when it goes from double support phase to single support phase, while

we should prevent it fall down forward in “inverse pendulum process” since it is close to the front edge of the supporting leg.

3.2 Stable Criteria with Energy Function for Lowering Down-Rising Up Process

In this process, we would imitate the human walking behavior. Observing from our walking behaviors, when we walk with the same pattern, the knee joint of the front leg would be locked all the time. However, if we want to accelerate our walking speed, we might change our walking pattern from the small step to the large step. In this situation, we would bend our knee joint of the front leg to lower down our center of mass naturally. Fig. 20 shows the behavior of human walking.

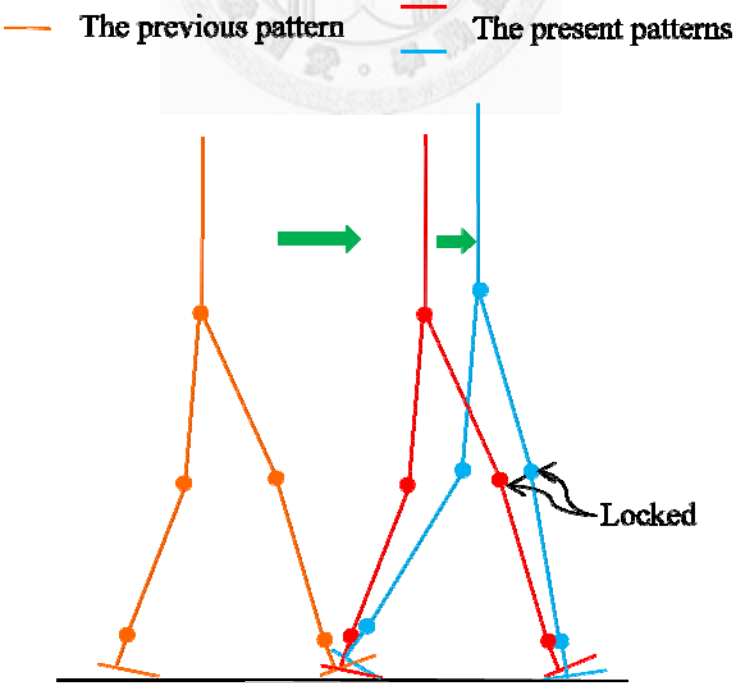

(a) Walking with the same pattern

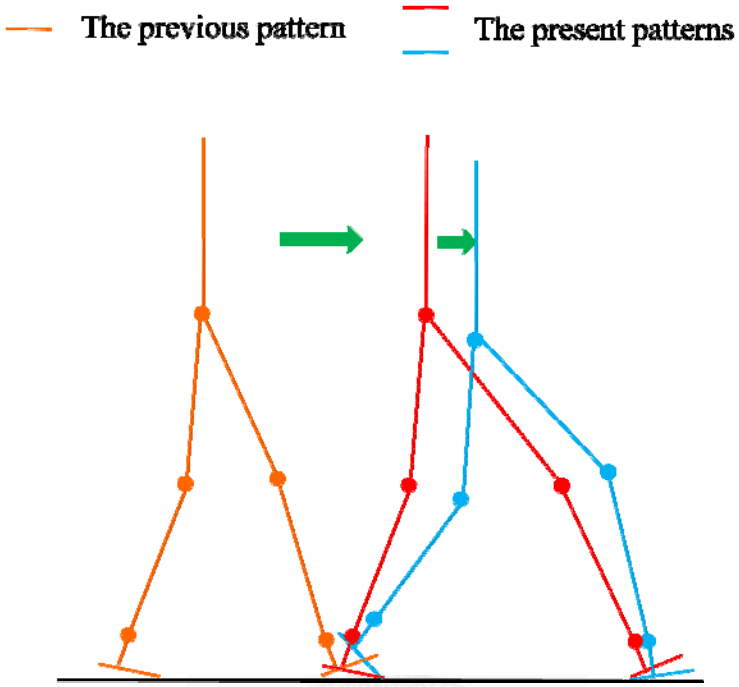

(b) Walking with changed patterns from the small one to the large one by bending our knee

Fig. 20. The behavior of human walking

3.2.1 Modeling for Interpreting Human Walking Behavior

Here, our objective is to figure out these natural walking behaviors, and to extract some useful information for our robot. Before we interpret these behaviors, we would make some assumptions to the humanoid model as follows, which would make us easier to figure out them:

(1) We neglect the foot of the model, so that the five links model would be used here.

(2) We assume the center of mass of the model is located at its hip.

(3) The time table of one step period is defined as follows (DSP means *Double*

Support Phase, while SSP means *Single Support Phase*.):

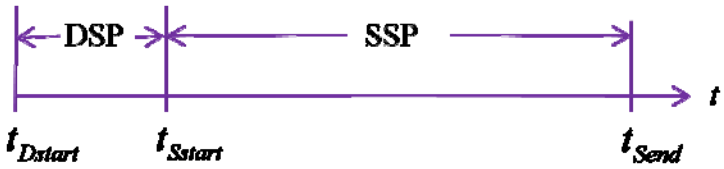

The model can be seen in Fig. 21, we would interpret the above two cases individually.

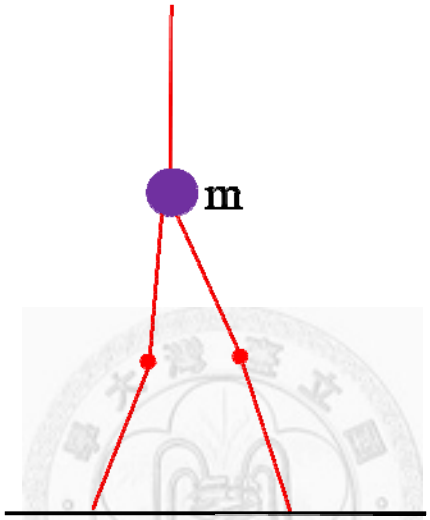

Fig. 21. The five links model for interpreting.

3.2.2 Case 1: Walking with the same pattern

When we walk with the same pattern, we usually lock the knee joint of the front leg in one walking period, such as Fig. 22.

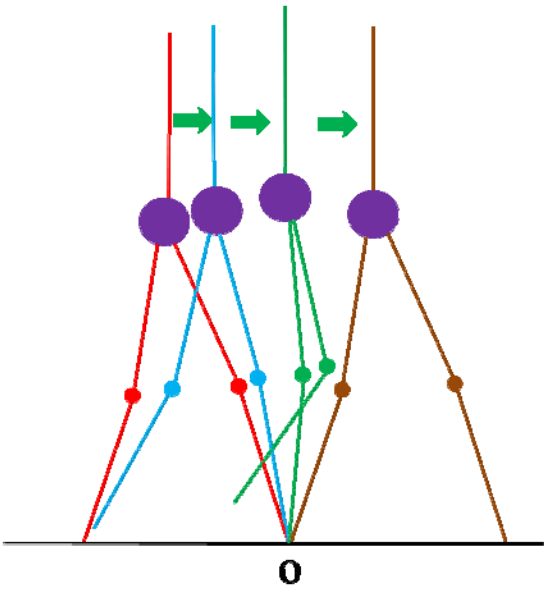

Fig. 22. One step of case 1

The model would rotate point O while walking. Therefore, point O is the fulcrum of the walking motion, and the free body diagram can be regarded as Fig. 23.

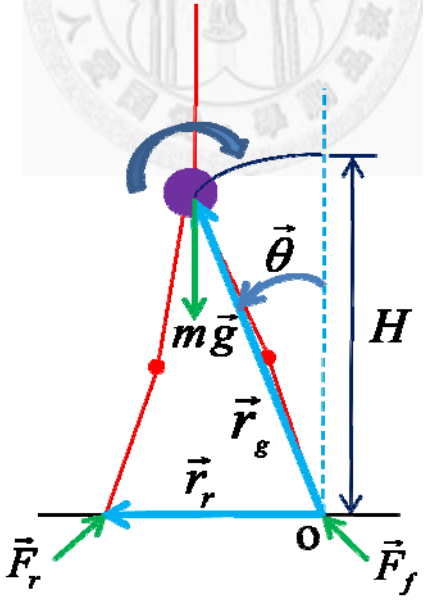

Fig. 23. The free body diagram of the model

According to the *Principle of Work and Energy*, the change of mechanical energy equals to the work done by all non-conservative forces. In our model, there exist two

non-conservative forces, which are $\vec{F}_r(\tau)$ and $\vec{F}_f(\tau)$, respectively, and $\vec{F}_f(\tau)$ does not do any work since it pass the fulcrum O. Therefore, we can write the mechanical energy function during one step as follows:

$$E_{me}(t) = E_{me}(t_{Dstart}) + \int_{\vec{\theta}(t_{Dstart})}^{\vec{\theta}(t)} [\vec{r}_r(\tau) \times \vec{F}_r(\tau)] \cdot d\vec{\theta}(\tau) \qquad (15)$$

Where $E_{me}(t_{Dstart})$ is the initial mechanical energy of one step, and $t_{Dstart} \le t < t_{Send}$. The term $\int_{\vec{\theta}(t_{Dstart})}^{\vec{\theta}(t)} [\vec{r}_r(\tau) \times \vec{F}_r(\tau)] \cdot d\vec{\theta}(\tau)$ means the work done by the ground reactive force of the rear leg $\vec{F}_r(\tau)$, and we need to notice that $\vec{F}_r(\tau)$ is only available in DSP, such as Eq.(16).

$$\left|\vec{F}_r(\tau)\right| = \begin{cases} f(\tau) \\ 0 \end{cases} \quad for \quad \begin{matrix} t_{Dstart} \le \tau < t_{Sstart} \\ t_{Sstart} \le \tau < t_{Send} \end{matrix} \qquad (16)$$

$$where \quad f(\tau) > 0$$

The rear leg can only do work in DSP, and the work must be a non-negative value since the term $\vec{r}_r(\tau) \times \vec{F}_r(\tau)$ has the same direction as $d\vec{\theta}(\tau)$ while walking forward. Eq.(17) shows the relationship of work in different time segment.

$$\begin{cases} [\vec{r}_r(\tau) \times \vec{F}_r(\tau)] \cdot d\vec{\theta}(\tau) \ge 0 \\ [\vec{r}_r(\tau) \times \vec{F}_r(\tau)] \cdot d\vec{\theta}(\tau) = 0 \end{cases} \quad for \quad \begin{matrix} t_{Dstart} \le \tau < t_{Sstart} \\ t_{Sstart} \le \tau < t_{Send} \end{matrix} \qquad (17)$$

However, the mechanical energy $E_{me}(t)$ must be periodic for every step while periodic walking. Accordingly, the term $[\vec{r}_r(\tau) \times \vec{F}_r(\tau)] \cdot d\vec{\theta}(\tau)$ must be zero for any time; Otherwise, $E_{me}(t)$ would not be periodic, and it will go to infinity when

$t \to \infty$ since there does not exist any term which can dissipate the energy in Eq.(15). Moreover, since the two terms $\vec{r}_r(\tau) \times \vec{F}_r(\tau)$ and $d\vec{\theta}(\tau)$ have the same direction and $d\vec{\theta}(\tau)$ would not be zero while walking forward, we can ascertain that $\vec{r}_r(\tau) \times \vec{F}_r(\tau)$ must be zero, which means that $\vec{F}_r(\tau)$ has no normal component. Therefore, without normal force, friction force would be zero, so the tangential component of $\vec{F}_r(\tau)$ must be zero since it is friction force. That is to say, $\left|\vec{F}_r(\tau)\right|$ is zero for any time, so we can guarantee that the duration of DSP ($t_{Dstart} \le \tau < t_{Sstart}$) would approach to zero from Eq.(16), which implies that in theory, when we walk with periodic pattern, only SSP is available. Therefore, Eq.(15) can be simplify into Eq.(18).

$$E_{me}(t) = E_{me}(t_{Dstart}) \qquad for \quad t_{Dstart} \le t < t_{Send} \qquad (18)$$

Eq.(18) describes that when we walk with periodic pattern, "*conservation of mechanical energy*" is used for any time.

In sum, when we walk with periodic pattern, the mechanical energy is conserved for any time, and only SSP is available in theory. However, in actual situation, there are some buffering elements in our body structure, such as gristles and foot arch, which is like the shock absorbers to absorb the vibration while walking, but they also dissipate a little mechanical energy of our body which is used for walking. Consequently, we need to supply a little mechanical energy which is dissipated by the buffering elements

every step. So the term $\int_{\vec{\theta}(t_{Dstart})}^{\vec{\theta}(t)} [\vec{r}_r(\tau) \times \vec{F}_r(\tau)] \cdot d\vec{\theta}(\tau)$ would not be zero, and therefore SSP would have a small duration. Note that the little supplying mechanical energy is converted from the chemical energy of our body, which means we only need to spend a little energy stored in our body to maintain the periodic walking every step.

Note that the above walking behavior of the model should accord with the following assumption:

$$E_{me}(t) \geq mgH \tag{19}$$

Otherwise, the model would fall down backward. Therefore, from the inspiration, we can define a parameter U_b as follows, which is call potential barrier:

The potential barrier U_b of a trajectory $Traj.(\vec{\theta}, |\vec{r}_g|)$ is the potential energy of the center of mass that passes through the vertical position $\theta = 0^\circ$ along the trajectory.

Fig. 24 shows the concept of potential barrier.

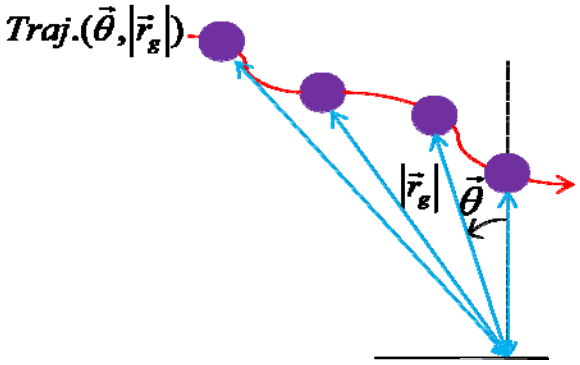

Fig. 24 The concept of potential barrier

We can also define the stable criteria of walking forward:

Assume the mechanical energy $E_{me}(t)$ *of the center of mass of the model is conserved along* $Traj.(\vec{\theta},|\vec{r}_g|)$ *during* $t_{Dstart} \le t < t_{Send}$ *of one step, and* $E_{me}(t)$ *should larger or at least equal to* U_b *; Otherwise, the model would fall down backward.*

That is, the stable criteria of walking forward written in mathematic form would be that:

$$E_{me}(t) \ge U_b \tag{20}$$

We would use this criterion to explain the following case.

3.2.3 Case 2: Walking with changed patterns from small one to large one

When we want to accelerate our walking speed by enlarging our walking pattern from the small step to the large step, from our observation, we would tend to bend our knee joint of the front leg to lower down our center of mass naturally, and then rise up to the original height, such as Fig. 25.

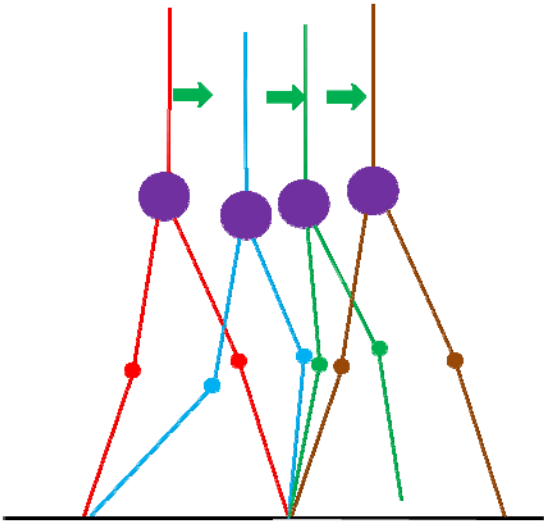

Fig. 25 One step of case 2

To illustrate this phenomenon, let us assume that we would preserve the mechanical energy from the previous (small) step in the large step. That is, there is no more mechanical energy converted from the chemical energy stored in our body because of changing step from smaller one to larger one. In fact, to preserve the mechanical energy, we can consider the model is like SLIP (Spring Loaded Inverted Pendulum) model [10] [11] [12] . In the model, the whole body would be simplified into a particle, and the legs would be considered as a spring to restore the mechanical energy, such as Fig. 26.

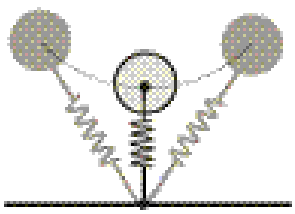

Fig. 26 Spring Loaded Inverted Pendulum Model

However, if we still want to lock our knee of front leg for large step, we would find that the potential barrier of large step is larger than small step, such as Fig. 27.

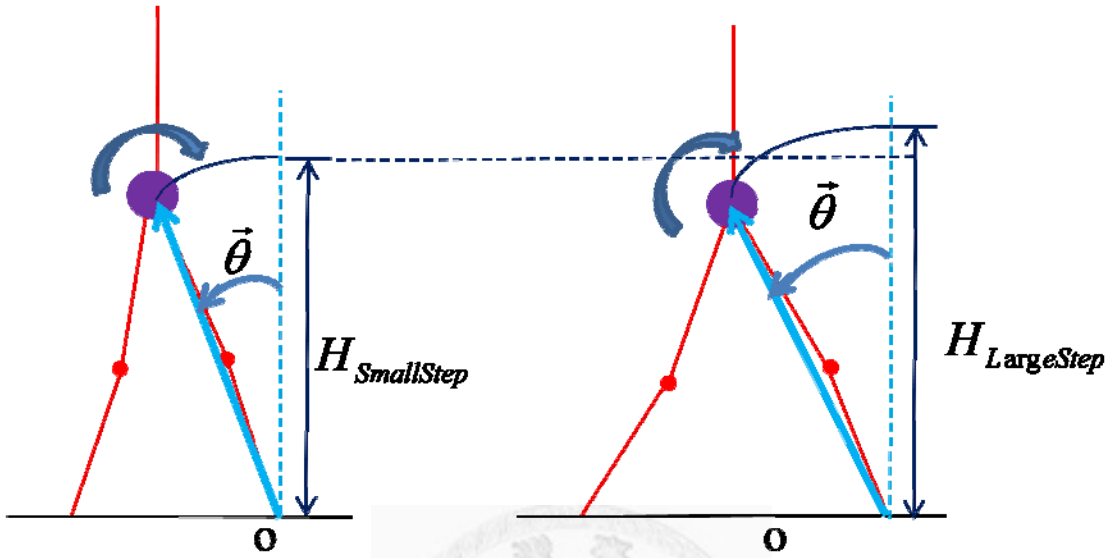

Fig. 27 Comparing the potential barrier between small step and large step

To finish the walking process, the mechanical energy preserved from the previous (small) step should accord with Eq.(20). However, from our assumption, it is the same as the small step. That is to say, from the degree of mathematics, we cannot ensure that it would accord with Eq.(20) since the potential barrier become larger in large step. Nevertheless, we have the sense of our own mechanical energy of our body and the potential barrier of the step we walked. We would first predict whether we can accord with Eq.(20) with locking the knee of front leg or not. If we predict that it would work, we would still walk with locking our knee of front leg, which is like in **Case 1**. Otherwise, we will bend the knee of the front leg to lower down our center of mass to decrease potential barrier, and then rise up to the original height such as Fig. 28 .

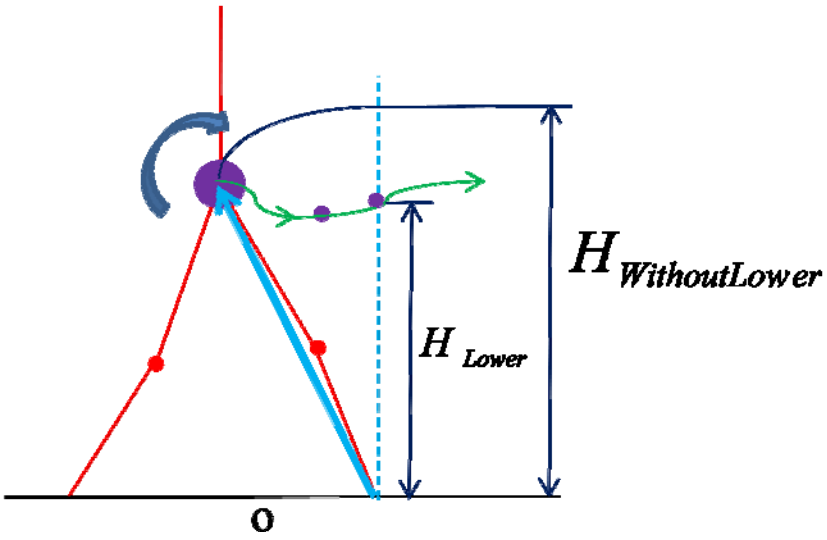

Fig. 28 Lower down to decrease potential barrier

Therefore, according to our explanation in theory, if we want to implement human-like walking on a biped robot, we can preset the mechanical energy of the center of mass of the robot, which would be preserved at the same value for all walking process, of course, it should accord with Eq.(20) of the trajectory of center of mass we plan. Then the robot would be able to walk.

However, there exist modeling errors between the model and actual biped robot such that we assume its center of mass is concentrated at its hip. That is, we cannot get the exact mechanical energy through the model, so we cannot ensure it would accord with Eq.(20).

Nevertheless, our explanation also imply that if we cannot ensure whether the mechanical energy is larger than the potential barrier, “lowering down-rising up” would be the conservative way for walking since it can decrease the potential barrier.

Therefore, to consider the problem, we would not follow the theoretical method totally, but keep the “lowering down-rising up” behavior.

3.2.4 Implementing Lowering Down-Rising Up Behavior for a Biped Robot

To implement “lowering down-rising up” behavior for a biped robot, we only need to choose three positions, which are initial position, end position and acme, and using spline curves to connect each other. By tuning the acme, we can get several trajectories with different potential barriers for center of mass. Fig. 29 shows this method.

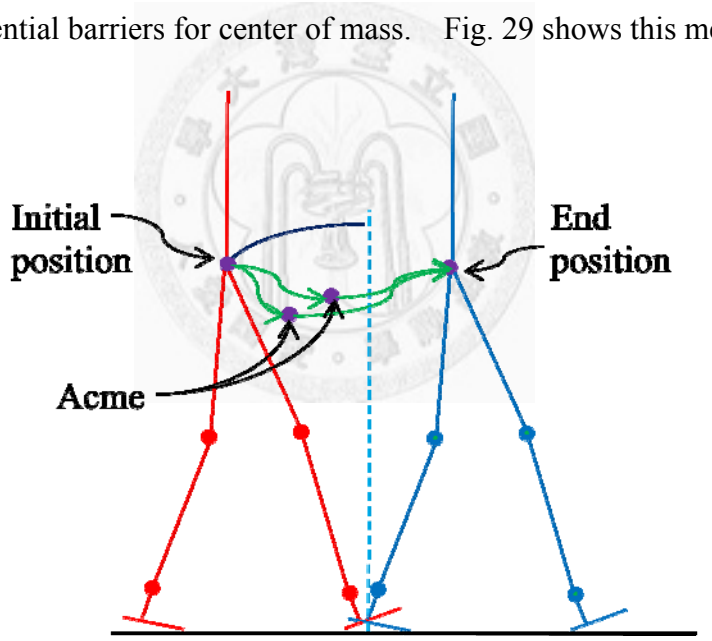

Fig. 29 Implementing “lowering down-rising up” behavior for biped robot

For tuning the position of acme, there is a useful tip that if the robot fall down backward, lowering and tuning the position of acme forward would amend the situation since this way would help the robot to decrease the potential barrier. Fig. 30 shows our description.

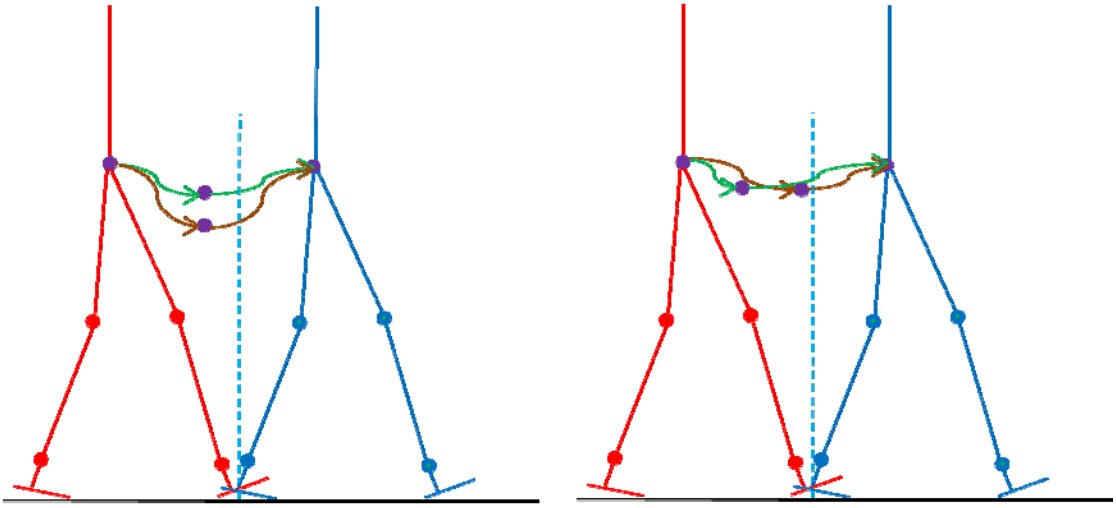

Fig. 30 Lowering and tuning the position of acme forward would decrease the potential barrier

In [13], we build a 2D robot for simulation to demonstrate this walking algorithm (Fig. 31). We use strait line to connect initial position, acme and end position to generate several trajectories, and then we use *Simulated Annealing* with one step time interval as its cost function to help us to select a stable trajectory for the robot. Fig. 32 shows the simulation result.

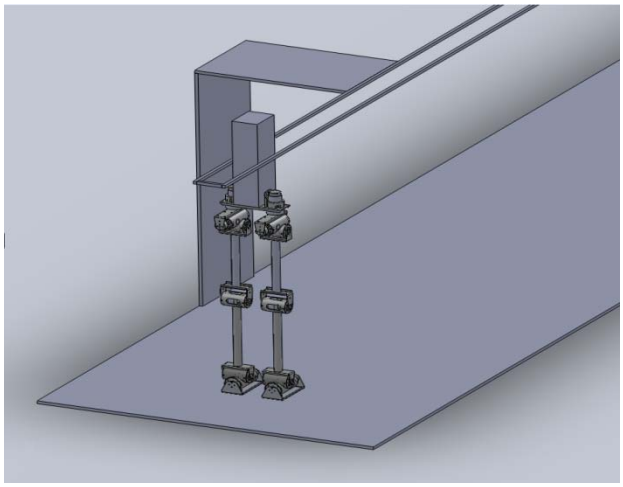

Fig. 31 The 2D robot for simulation

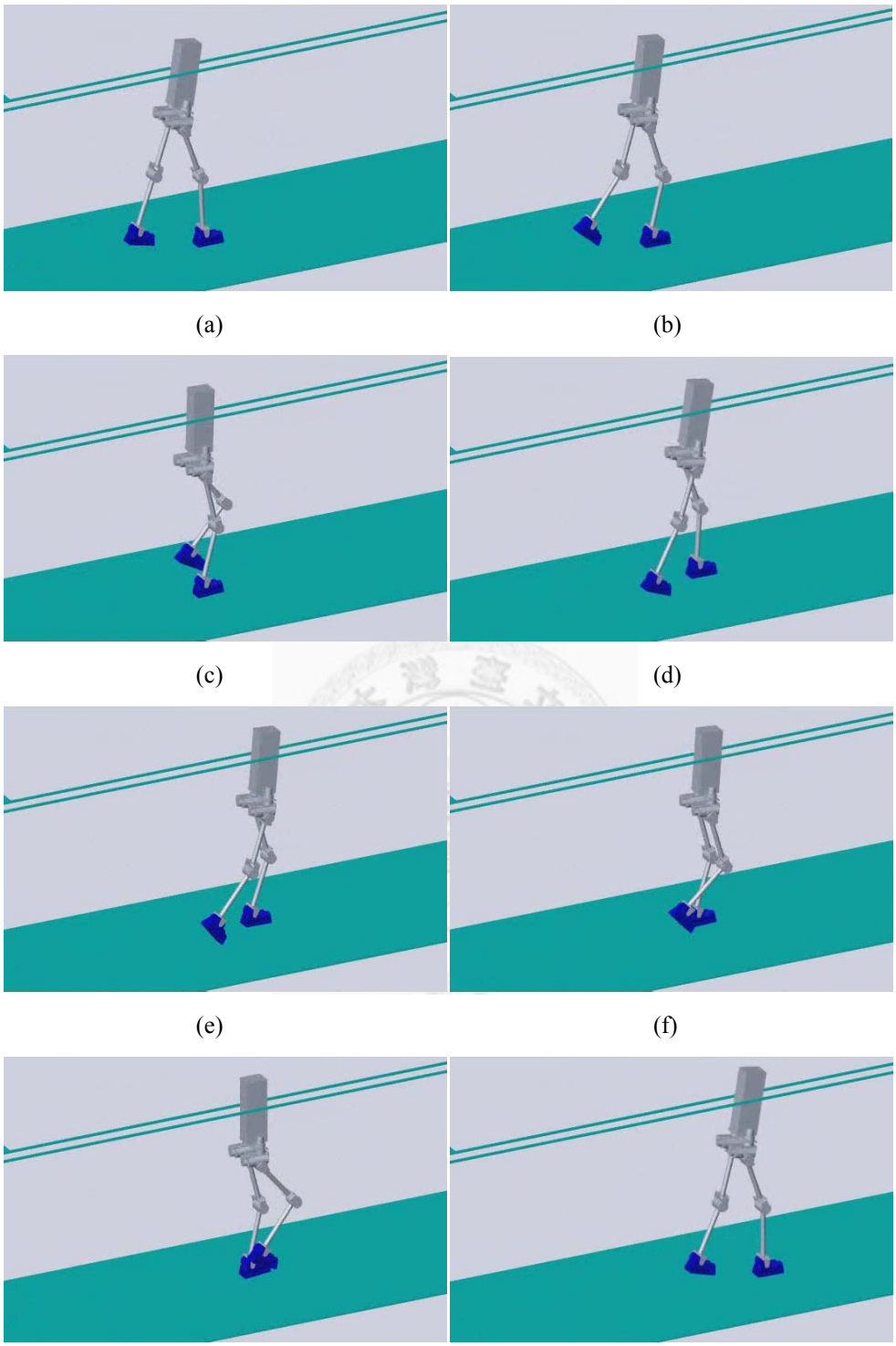

(a) (b)

(c) (d)

(e) (f)

(g) (h)

Fig. 32 Simulation for walking algorithm

3.3 Stable Criteria with ZMP for Inverse Pendulum Process

By tuning the acme position in lowering down-rising up process, we have our robot overcome the potential barrier, which would enable our robot to have human-like walking and prevent it falling down backward. However, that process could not ensure the robot not to fall down forward. Consequently, to prevent the robot from falling down forward, ZMP concept would be used in inverse pendulum process. In this process, we would generate the stable hip trajectory by keeping the position of ZMP, r in the foot polygon.

3.3.1 Modeling for Inverse Pendulum Process

In this process, we would make some assumptions as follows:

(1) The whole mass of the robot is concentrated on its hip donated as m, and it is supported by the foot of the supporting leg, which is in static equilibrium, and the knee joint of the supporting leg do not rotate during inverse pendulum process for keeping L to be constant.

(2) For convenient to solve the dynamic equation, we assume θ is small, and the mass center does not move drastically at vertical direction. Therefore, we would neglect its nonlinear terms. i.e. vertical acceleration $a_y \cong 0$, $\sin\theta \cong \theta$, $\cos\theta \cong 1$, $\dot{\theta}^2 \cong 0$.

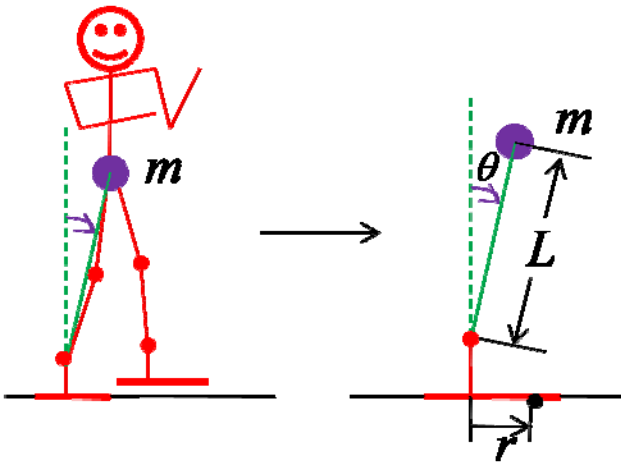

Fig. 33 Modeling for inverse pendulum process

3.3.2 Derivation for Hip Trajectory

To derive the hip trajectory of the robot, we first take the free body diagram of its foot of supporting leg to get Eq.(21):

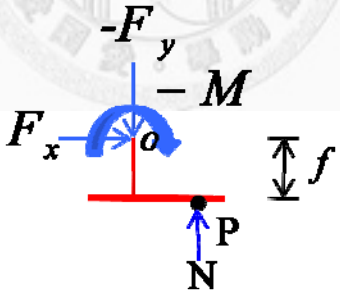

Fig. 34 Free body diagram of the robot's foot of supporting leg

$$\circlearrowleft \sum M_p = 0 \Rightarrow -(-F_y r) + (-M) + (-F_x f) = 0$$

$$r = \frac{M + F_x f}{F_y} \tag{21}$$

Where r is the desire ZMP position. M, F_x and F_y are joint torque and joint

reactive force. Then we take the free body diagram of the inverse pendulum part to get Eq.(22), Eq.(23), Eq.(24):

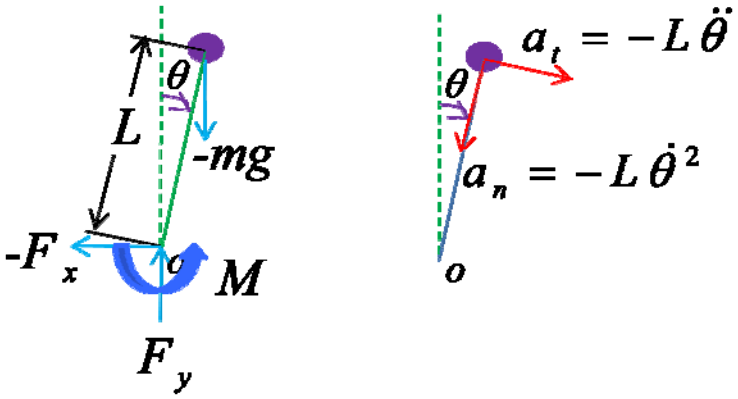

Fig. 35 Free body diagram of the inverse pendulum part

$$\oplus \sum M_o = I\alpha \Rightarrow M + mgL\sin\theta = mL^2\ddot{\theta}$$
$$\Rightarrow M = mL^2\ddot{\theta} - mgL\sin\theta \qquad (22)$$

$$+\rightarrow \sum F_y = ma_y \Rightarrow F_y + (-mg) \cong 0$$
$$\Rightarrow F_y = mg \qquad (23)$$

$$+\rightarrow \sum F_x = ma_x \Rightarrow -F_x = m\cdot(a_{tx} + a_{nx})$$
$$= m\cdot[a_t\cos\theta + (-a_n\sin\theta)]$$
$$= m\cdot(-L\ddot{\theta}\cos\theta + L\dot{\theta}^2\sin\theta)$$
$$\Rightarrow F_x = mL\ddot{\theta}\cos\theta - mL\dot{\theta}^2\sin\theta \qquad (24)$$

By Combine Eq.(22), Eq.(23), Eq.(24) and Eq.(21), we can get Eq.(25) as follows:

$$r = \frac{mL^2\ddot{\theta} - mgL\sin\theta + (mL\ddot{\theta}\cos\theta - mL\dot{\theta}^2\sin\theta)f}{mg} \quad (25)$$

From our assumption that, we can simplify Eq.(25) into Eq.(26):

$$r = \frac{mL^2\ddot{\theta} - mgL\theta + mfL\ddot{\theta}}{mg}$$

$$= (\frac{L^2 + fL}{g})\ddot{\theta} - L\theta \quad (26)$$

Let $\alpha = (\frac{L^2 + fL}{g})$, Eq.(26) becomes Eq.(27):

$$\alpha\ddot{\theta} - L\theta = r \quad (27)$$

In inverse pendulum process, we would like to keep ZMP at the same position. Therefore, we can set r *to be a constant, and then solve Eq.(27). We can get Eq.(28):*

$$\theta(t) = C_1 e^{\sqrt{\frac{L}{\alpha}}\cdot t} + C_2 e^{-\sqrt{\frac{L}{\alpha}}\cdot t} - \frac{r}{L} \quad (28)$$

Taking the desire posture $\theta(T_d + T_u)$ and $\theta(T_d + T_u + T_i)$ as boundary condition,

such as Fig. 36, we can solve C_1 and C_2, and put them into Eq.(28) to get complete $\theta(t)$. In Fig. 37, we take $L = 59.943\text{cm}$, $f = 11.5\text{cm}$, $\alpha = 4.37\text{cm}\cdot\text{s}^2$, and use $\theta(0.75) = 0$, $\theta(1) = -10$ as the boundary condition. Then take $r = 2, 0, -5\text{cm}$ as three different cases to solve C_1 and C_2. After solving them in each case, we plot $\theta(t)$ versus t with each r for comparing.

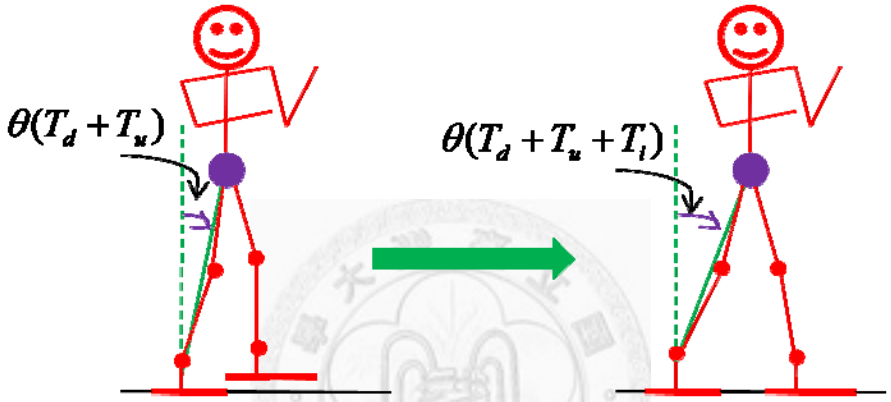

Fig. 36 The two desired postures $\theta(T_d + T_u)$ and $\theta(T_d + T_u + T_l)$.

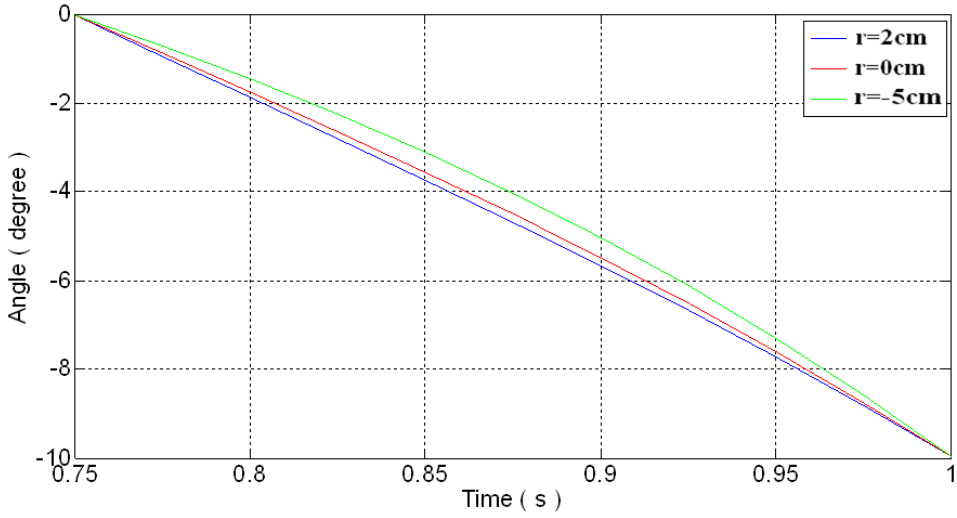

Fig. 37 The plot of $\theta(t)$ versus t with each r.

3.3.3 Implementing Inverse Pendulum Behavior for a Biped Robot

In theory, we can keep ZMP at the same position in the foot polygon by Eq.(28).

However, since there might exist some modeling errors or assumptions that do not coincide with the actual biped robot, it is impossible to keep ZMP at the same position. That is to say, if we try to keep ZMP at the same position in the foot polygon, ZMP might go out of the foot polygon during the inverse pendulum process, which means the biped robot would be unstable and falls down forward.

Nevertheless, although we cannot keep ZMP at the same position during the inverse pendulum process, it is possible to keep ZMP in the foot polygon during the process. We can assume that there exists some positions which we try to keep ZMP at one of them would make ZMP go out of the foot polygon during this process, donated as unstable positions, while other positions, donated as stable positions, would make ZMP still in the foot polygon during this process if we try to keep ZMP at one of them. Fig. 38 shows the concept of stable and unstable positions. (We try to keep ZMP at a position means, in Eq.(28), we let r' be the value of the position, and solve it.)

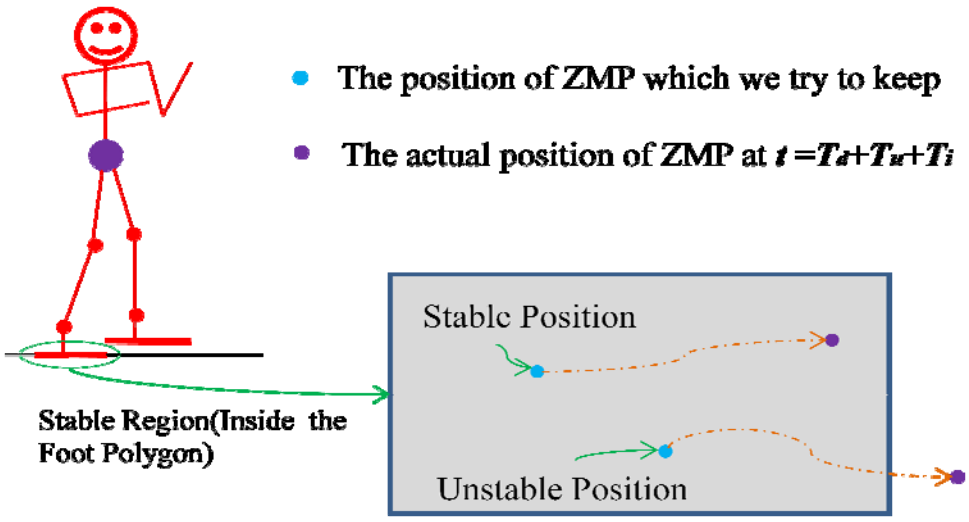

Fig. 38 The illustration of stable and unstable positions

To find the stable position for the actual biped robot, we do not need to feedback the actual positions of ZMP. We only need to set r to be an arbitrary value first (of course the value represents an arbitrary position in the foot polygon), and see whether the biped robot falls down or not. If the robot doesn't fall down, we can ascertain that the position we try to keep is a stable position; otherwise, it is a unstable position, and we need to pull the value of r backward until it is a stable position.

To verify the above tuning rule, we make an experiment in simulation. In Fig. 39, the value r is set to be 2 cm, and we run the simulation. From our simulation, the robot falls down forward. Therefore, r =2 cm is an unstable position. To make the robot stable while walking, in Fig. 40, we pull the value r backward from 2cm to -5 cm, and the robot can realize stable walking. Therefore, r =-5 cm is a stable position.

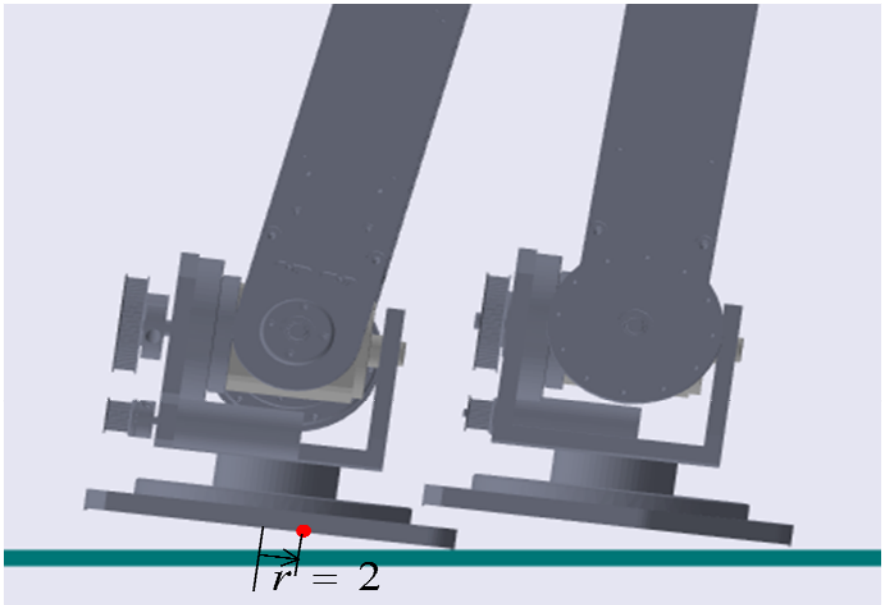

Fig. 39 The robot falls down forward while r=2cm, which is an unstable position.

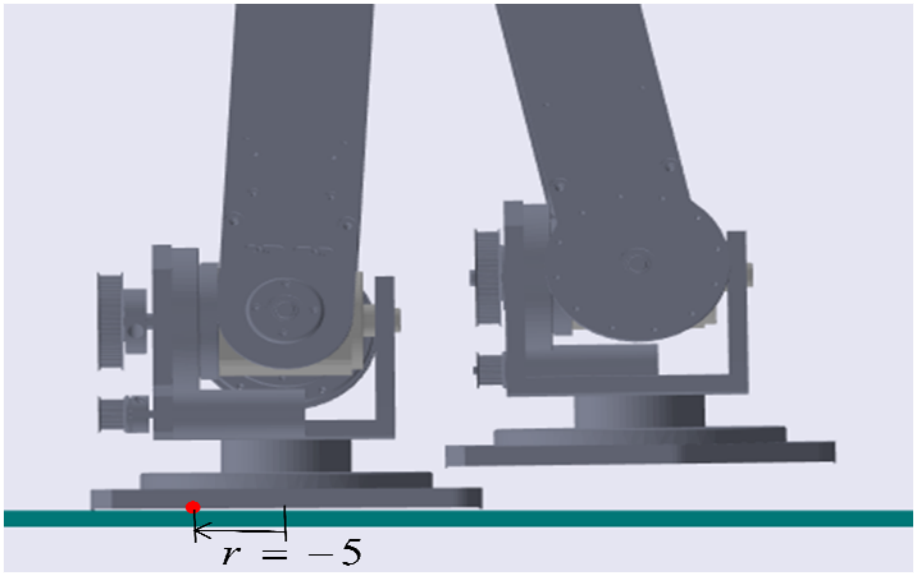

Fig. 40 The robot walks stably since we pull r backward from 2cm to -5cm, which is a stable position

3.4 Combination of Lowering Down-Rising Up Process and Inverse Pendulum Process

To implement a complete walking, we need to combine the two processes we mentioned. Fig. 41 shows the whole walking processes.

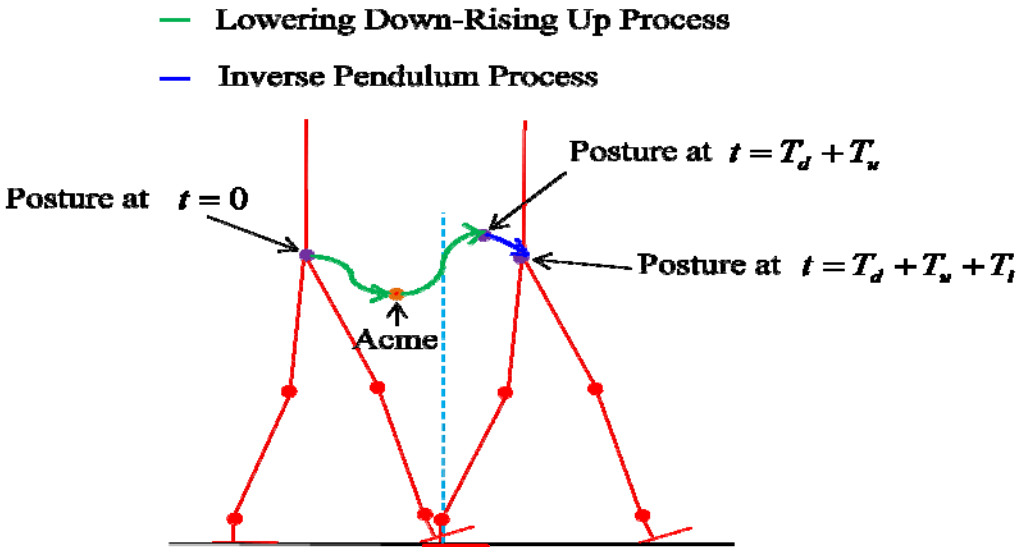

Fig. 41 The whole walking processes

To realize the whole processes, there are two steps we need to do. The first step is to choose the desire postures at $t = 0$, $t = T_d + T_u$ and $t = T_d + T_u + T_i$, which depend on walking step length. Then the other step is to find the proper parameters of stability, which are position of acme in lowering down-rising up process and the position of ZMP r which we try to keep in inverse pendulum process. To find the two parameters, we can establish some automatic tuning methods such in [13], which always include a cost function that we design and an optimizing method such as Simulated Annealing, Genetic Algorithm or Particle Swarm Optimizing Algorithm, or we can following the tuning rules that we mentioned in **Chapter 3.2.4** and **Chapter 3.3.3**. We first tune the parameters until the robot in simulation can walk, and then apply these simulation refined parameters to the actual biped robot. Although these parameters had been refined in simulation, we might still need to tune them slightly for the actual biped since there might exist some modeling difference in the simulation and the actual robot. Fig. 42 is the flow char of our tuning process. Finally, we present an example of the hip trajectory of one cycle generated by the trajectory generator (Fig. 43).

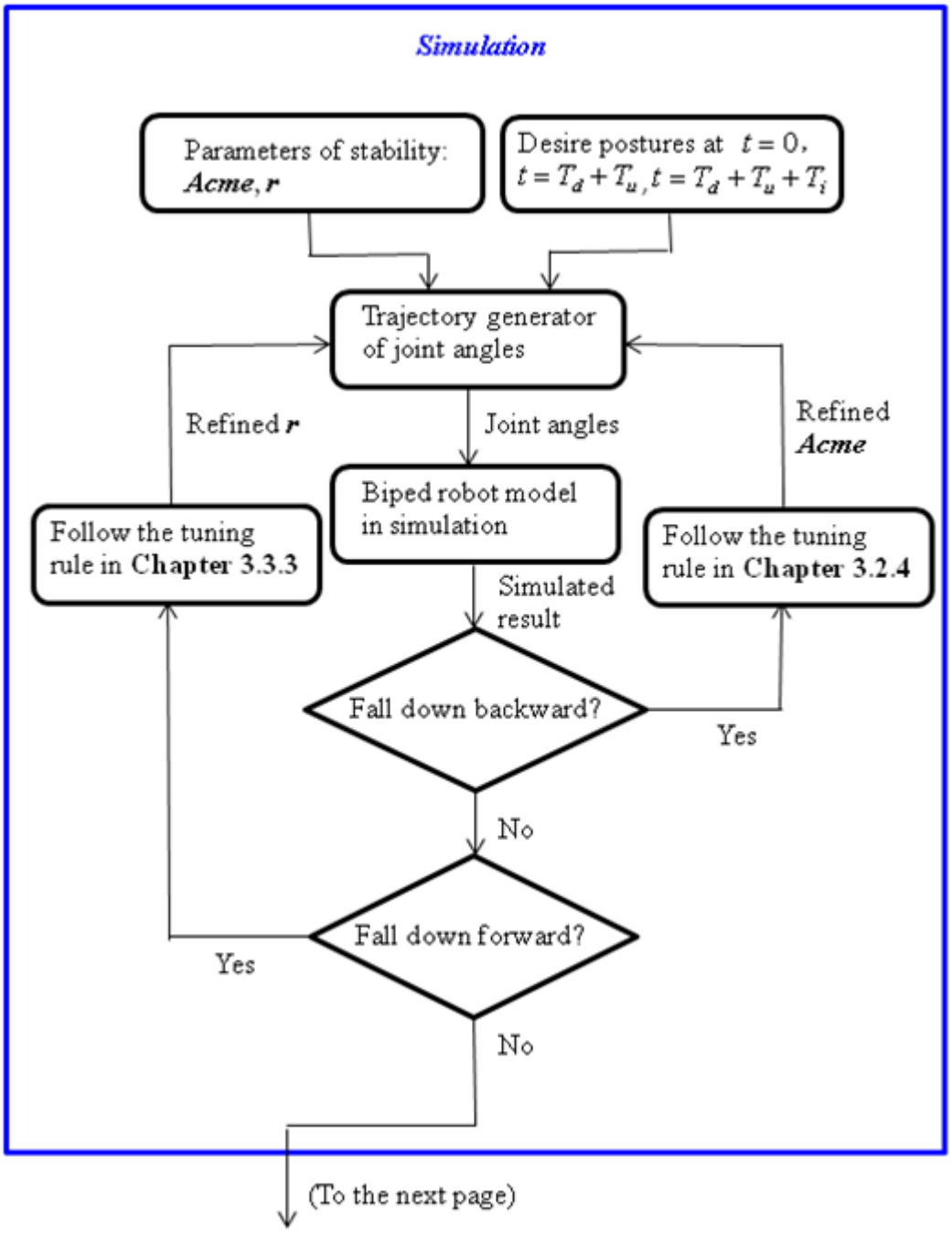
Simulation
Parameters of stability:
Acme, r
Desire postures at t = 0,
t = T_d + T_u, t = T_d + T_u + T_i
Trajectory generator
of joint angles
Refined r
Joint angles
Refined
Acme
Biped robot model
in simulation
Follow the tuning
rule in Chapter 3.3.3
Follow the tuning
rule in Chapter 3.2.4
Simulated
result
Fall down backward?
Yes
No
Fall down forward?
Yes
No
(To the next page)

(a)

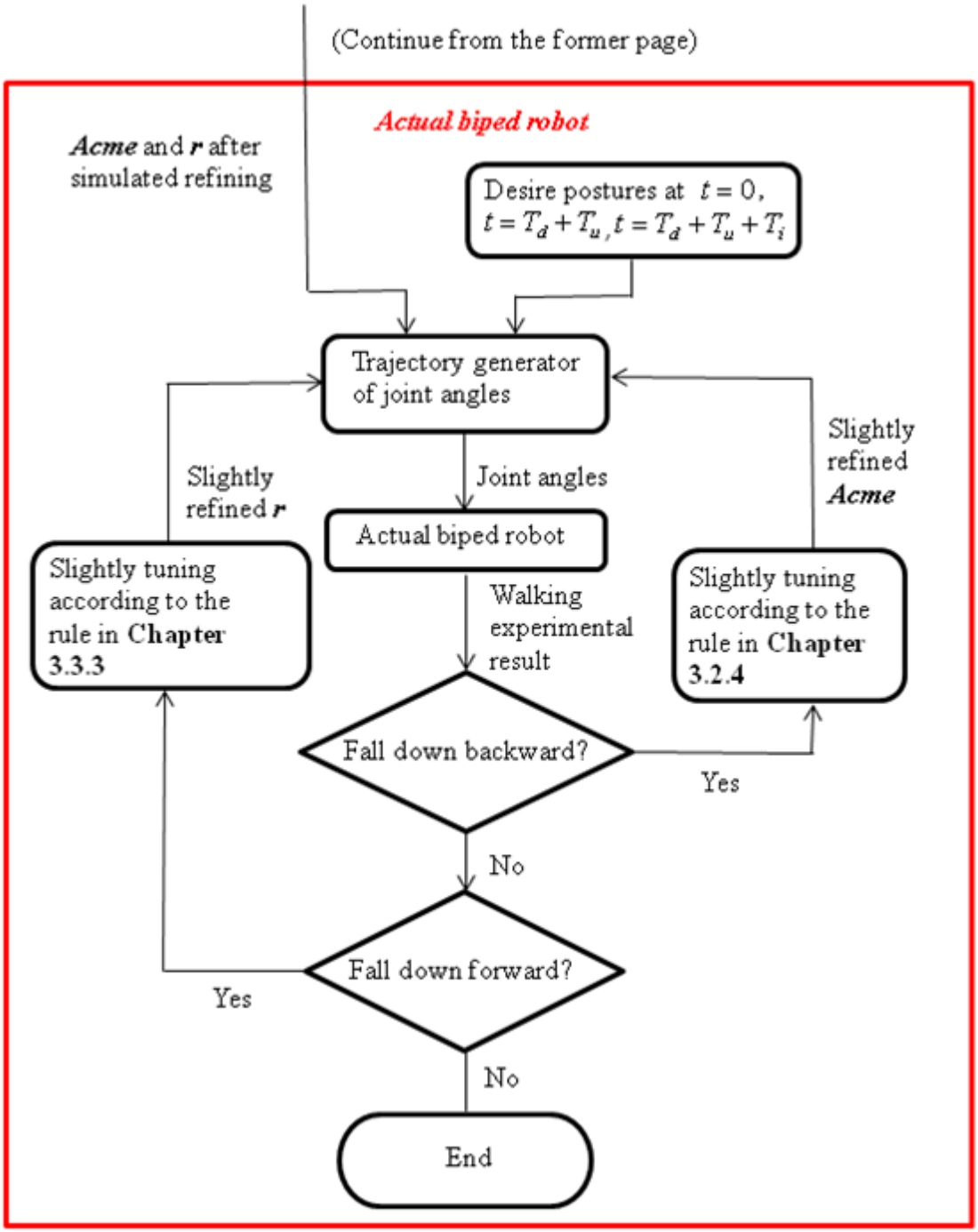

(b)

Fig. 42 Flow char of the tuning process

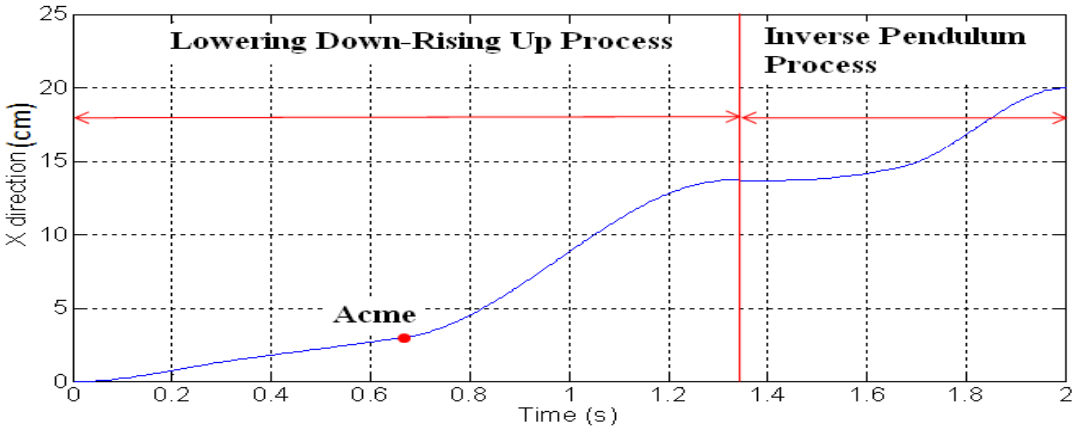

(a) X direction VS Time.

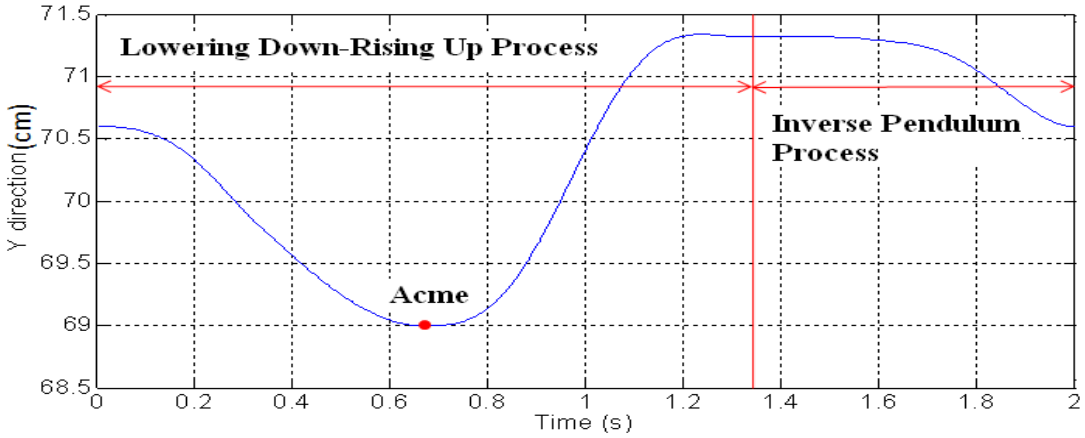

(b) Y direction VS Time.

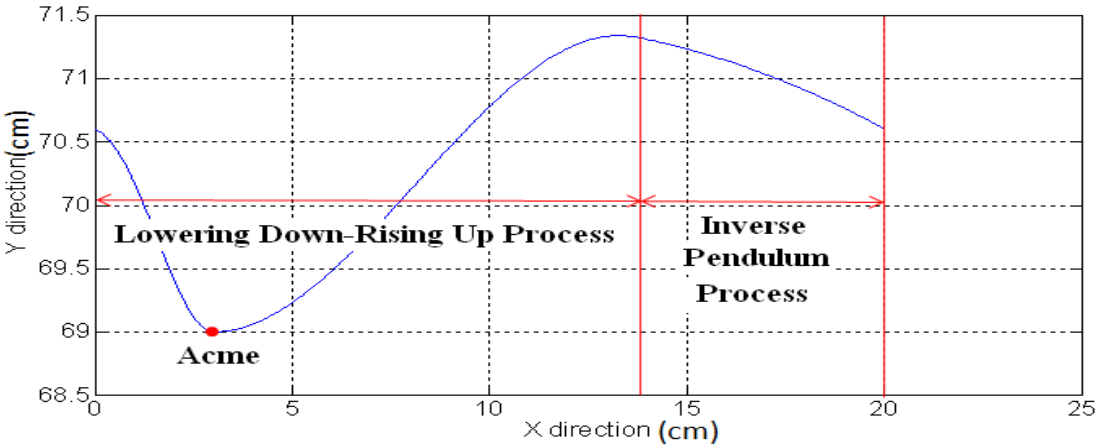

(c) X direction VS Y direction.

Fig. 43 An example of the hip trajectory of one cycle with Acme (3cm, 69cm), r=2cm.

Chapter 4 SIMULATION RESULTS AND EXPERIMENTATION ON WALKING

In this chapter, we will show two kinds of results. The first result is simulation result, while the other result is walking experiment of the actual biped robot.

From our walking algorithm, by tuning *Acme* and r, we realize three stable patterns with different step length and time. In Fig. 44, the pattern with 15 centimeter step length and 2 second step time is shown, which would also be applied on our actual biped robot (Fig. 47), and we also show the joint angles of the walking pattern generated by the trajectory generator (Fig. 48). In Fig. 45 and Fig. 46, we show the patterns with 20, 30 centimeter step length and 1 second step time. In the two patterns, the "hill contact- toe off motion" would be realized. However, we do not apply the two patterns to our actual biped robot since the tracking accuracy of each joint of our robot might not be enough. To realize the two patterns in the future, we improve the tracking ability of each controller, and the actual methods to improve it are discussed in **Chapter 6**.

The following are the illustrations of each figure from (a) to (h):

(a) The robot starts to enter "lowering down-rising up process".

(b) The robot is in "lowering down-rising up process".

(c) "Lowering down-rising up process" ends, and the robot starts to enter "inverse

pendulum process".

(d) The swing leg touches ground, and "inverse pendulum process" is finished. "Lowering down-rising up process" of the next walking step would be started.

(e) The robot is in "lowering down-rising up process".

(f) The robot is in "lowering down-rising up process".

(g) "Lowering down-rising up process" ends, and the robot starts to enter "inverse pendulum process".

(h) The swing leg touches ground, and "inverse pendulum process" is finished.

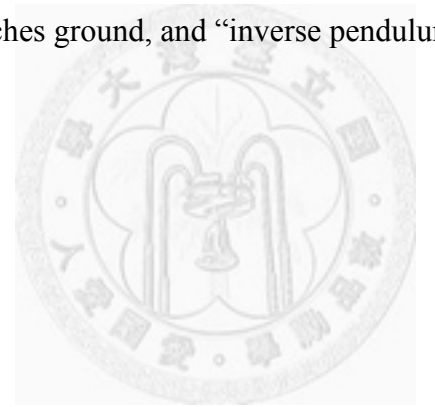

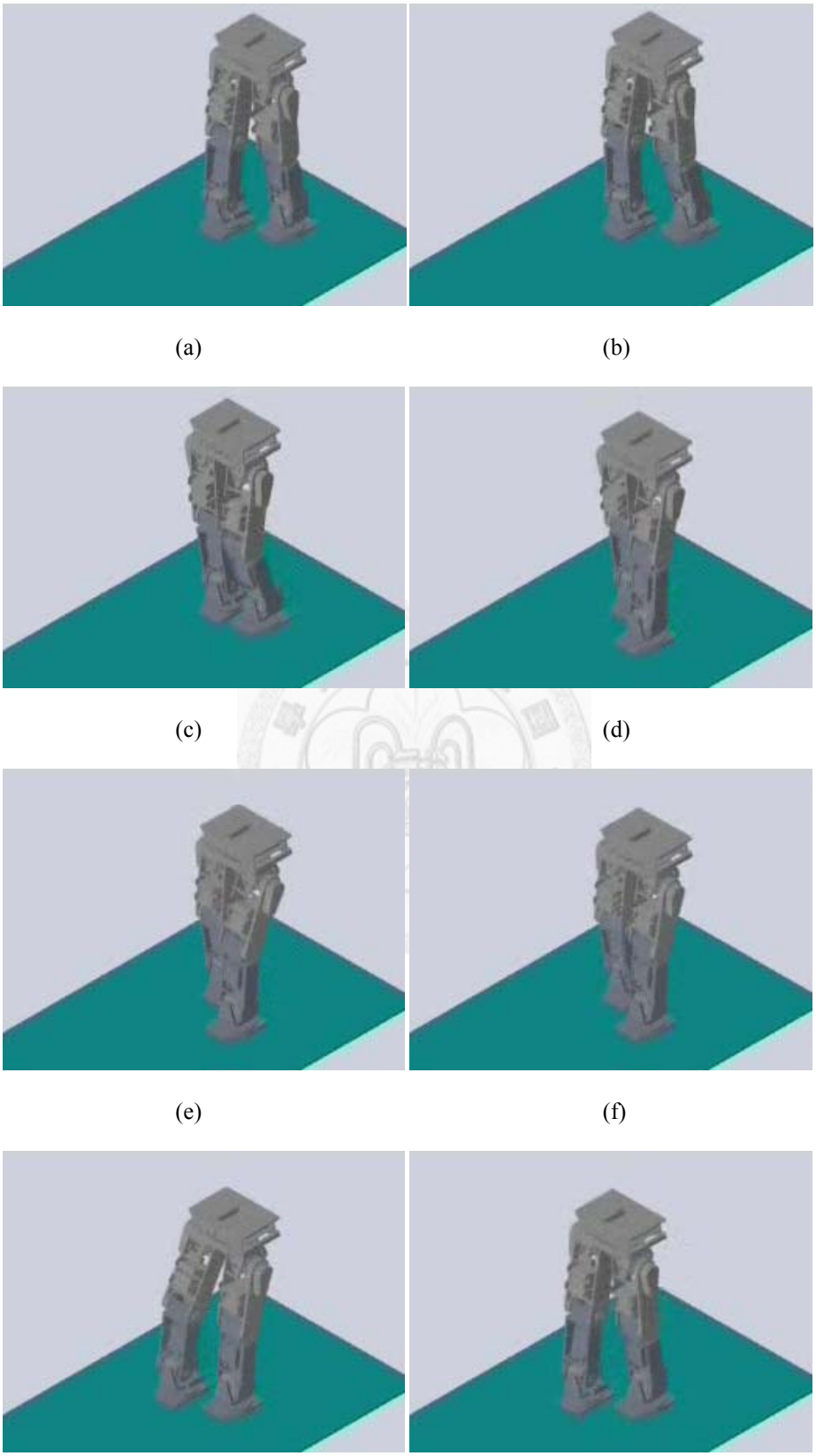

(a) (b)

(c) (d)

(e) (f)

(g) (h)

Fig. 44 Simulation of the walking pattern with step length: 15cm, step time: 2s, walking velocity: 7.5 cm/s, acme: (3cm, 70.5cm) and r: -8cm.

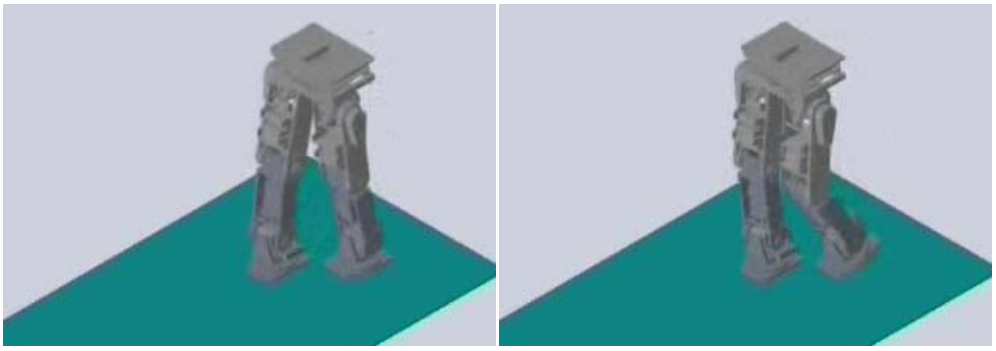

(a) (b)

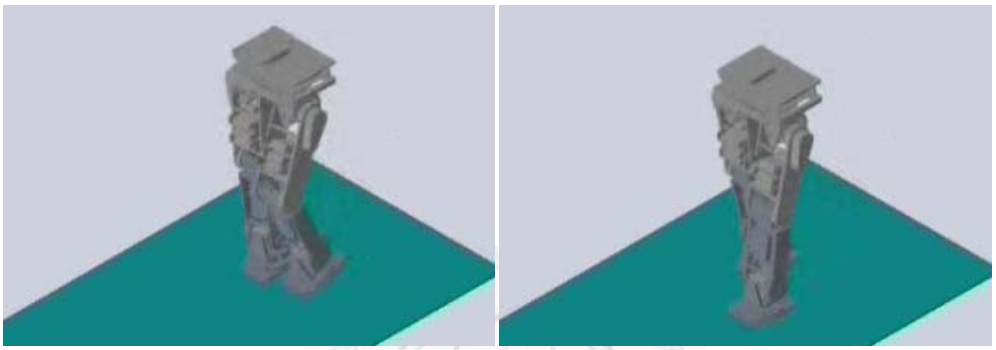

(c) (d)

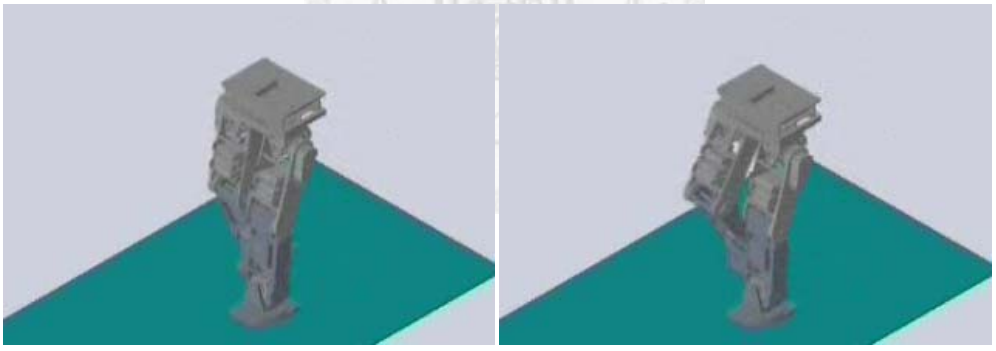

(e) (f)

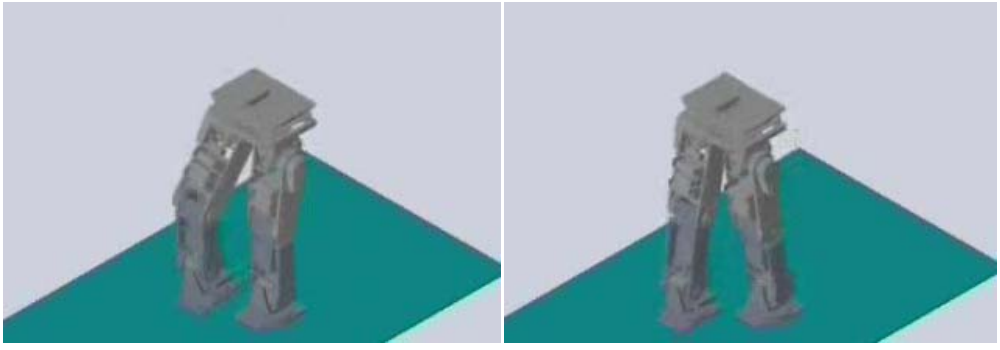

(g) (h)

Fig. 45Simulation of the walking pattern with step length: 20cm, step time: 1s, walking velocity: 20 cm/s, acme: (5cm, 71cm) and r: -5cm.

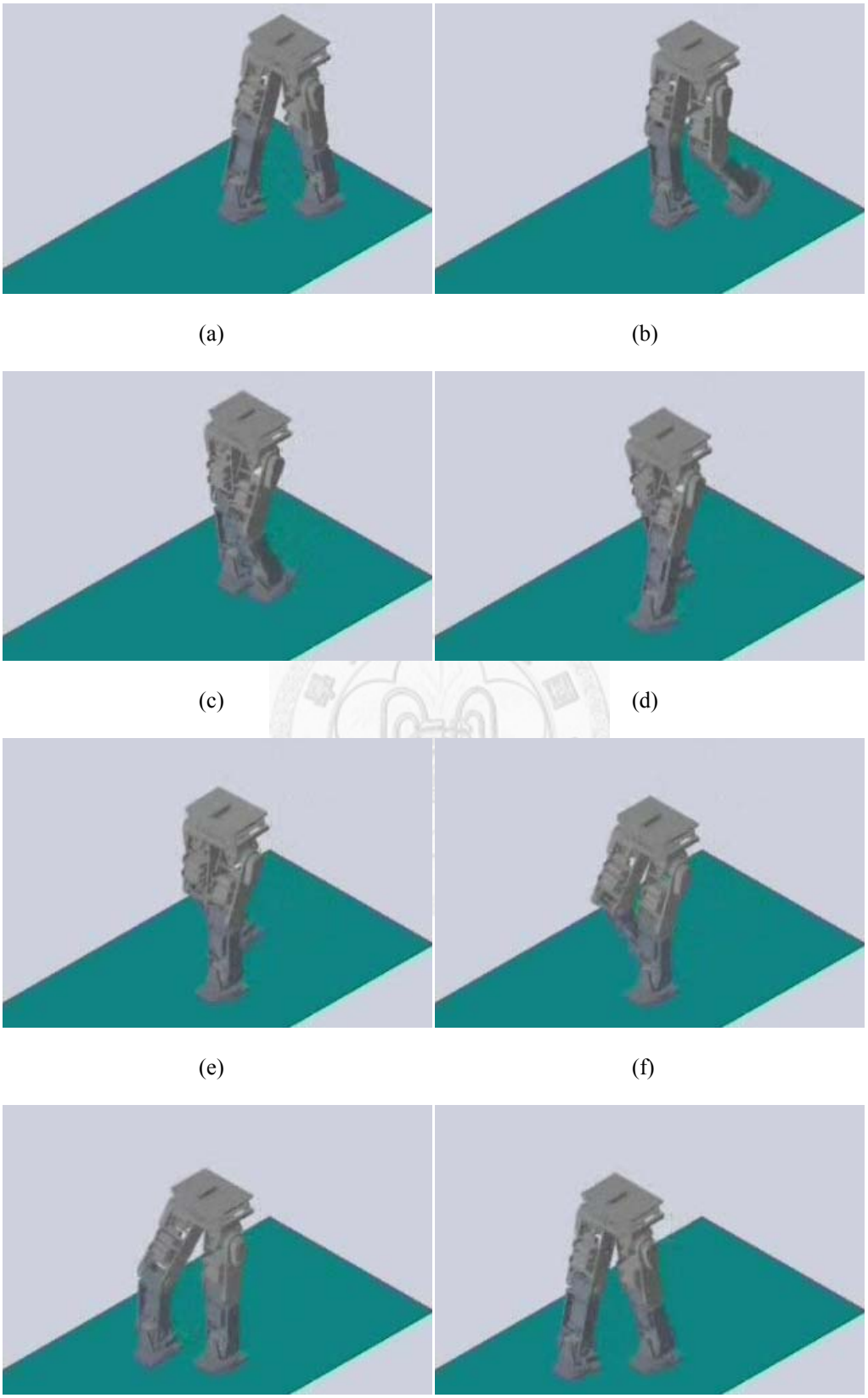

(a) (b)

(c) (d)

(e) (f)

(g) (h)

Fig. 46 Simulation of the walking pattern with step length: 30cm, step time: 1s, walking velocity: 30 cm/s, acme: (5cm, 69.5cm) and r: -5cm.

(a)

(b)

(c)

(d)

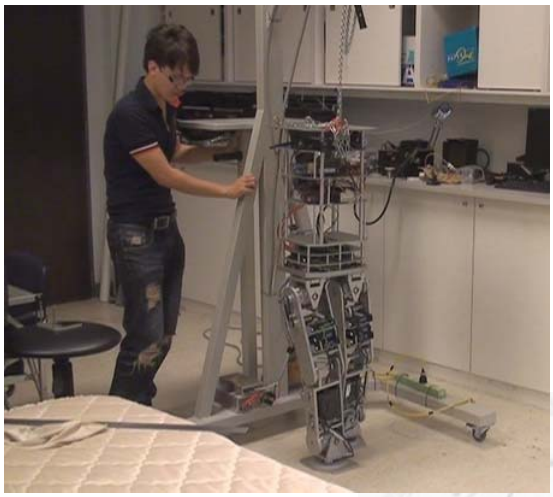

(e)

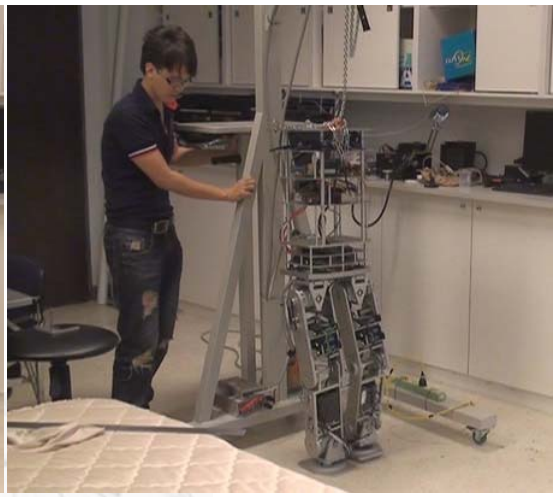

(f)

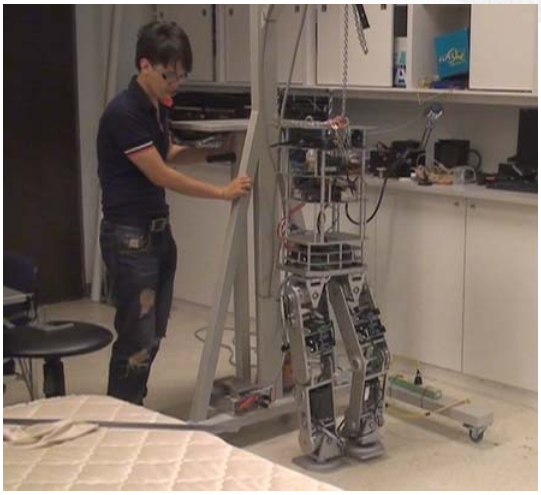

(g)

(h)

Fig. 47 Walking experiment with step length: 15cm, step time: 2s, walking velocity: 7.5 cm/s, acme: (3cm, 70.5cm) and r: -8cm.

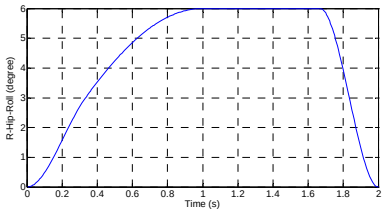

(a) R_Hip_Roll

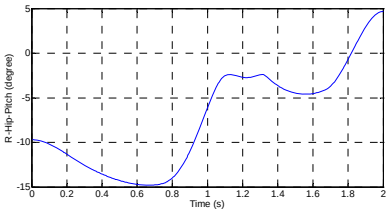

(b) R_Hip_Pitch

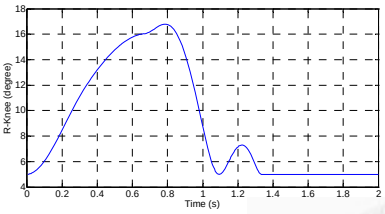

(c) R_Knee

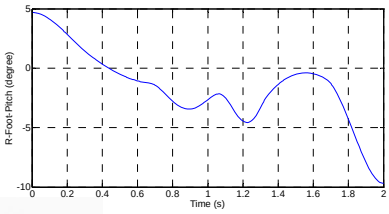

(d) R_Foot_Pitch

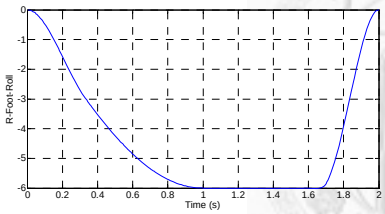

(e) R_Foot_Roll

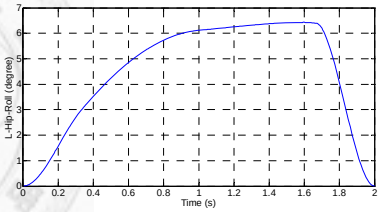

(f) L_Hip_Roll

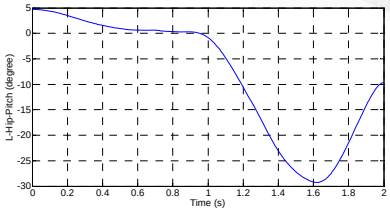

(g) L_Hip_Pitch

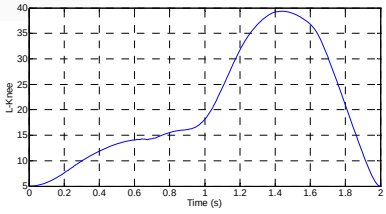

(h) L_Knee

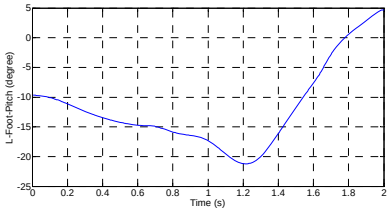

(h) L_Foot_Pitch

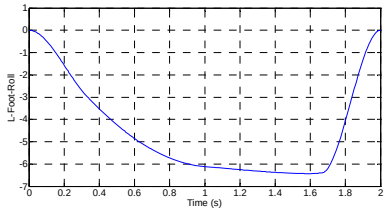

(i) L_Foot_Roll

Fig. 48 Joint angles of the walking pattern with step length: 15cm, step time: 2s.

Chapter 5 CONCLUSION AND CONTRIBUTIONS

In many literatures, for controlling the walking stability of the robot, the hip trajectory is planned at the same height, so the knees of the robot would bend while walking. However, this does not make sense when humans walk.

To deal with the problem, in this thesis, we develop a walking pattern generating algorithm. From our walking pattern generating algorithm, we can generate several stable walking patterns, and apply them to our physical model in simulation and actual biped robot to verify these patterns.

The main contributions of this thesis are following:

(1) Since the height of the hip is time varying, the knee can stretch at final posture of one step. This is especially different from a robot based on traditional walking patterns, which always bends its knee to maintain the hip at the same height.

(2) In tradition, if a robot is based on ZMP criteria, it needs sensors to feedback the actual ZMP position to adjust its posture to maintain its walking stability. However, in this thesis, to make a robot walk, we don't have to feedback the actual ZMP position. One thing we have to do is to notice the robot falls down forward or backward, and then follow the

tuning rule in **Chapter 3.2.4** and **Chapter 3.3.3** to tune the parameters of stability (*Acme* and *r*).

As a result of this thesis research, two papers have been published, which are listed as follows:

1. *R.C. Luo, IEEE, H.Y Chang ,and J.W Chen,* "The development of fuzzy virtual spring-damper generator for reducing biped walking contact vibration", 2010 Advance Robotics and its Social Impacts, Seoul, Korea.
2. *R. C. Luo, H. Y. Chang, H. H. Chang and Y. P. Yang,* "Walking Pattern Based on Simulated Annealing for Biped Robotics", 2011 IEEE World Congress on Intelligent Control and Automation, Taipei, R.O.C..

Chapter 6 FUTURE WORKS

Although we already generate several walking patterns, we do not apply total patterns to our actual biped robot since the tracking ability of each joint controller is not enough to track all patterns we feed to the controller, especially higher speed patterns. To realize the high speed patterns on our actual biped robot, we should improve its tracking ability of each joint controller. In this thesis, we just use PID (Proportional, Integral and Derivative) control for our biped robot, and it is hard to tune a set of proper PID gain for the entire walking processes since the external torques due to gravity are time varying. Therefore, a feasible method to enhance the tracking ability of controller is to eliminate the effect of gravity. That is, **Gravity Compensation Algorithm** would be added to the joint controllers to eliminate the influence of gravity in the future. Besides, **Adaptive Impedance Control Algorithm** would also be applied to controller to replace the simple PID control (Fig. 49). In the future, we might see the robot walks with high speed after enhancing the tracking ability of each controller.

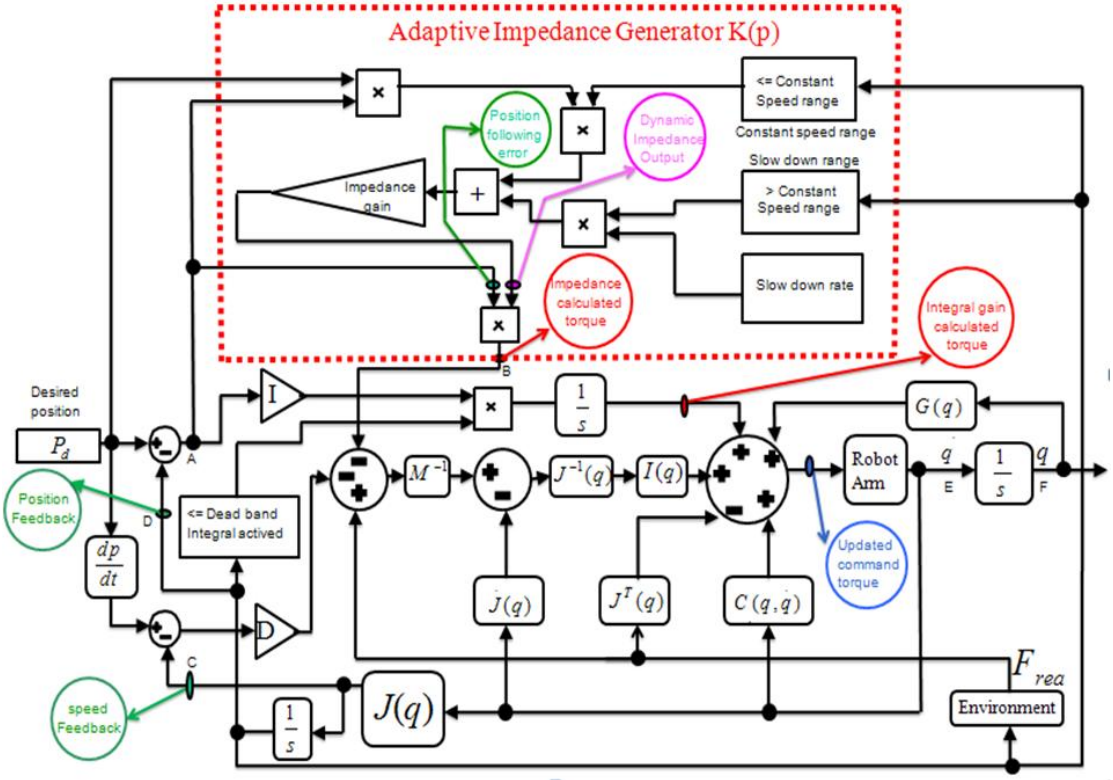

Fig. 49 Block diagram of Adaptive Impedance Control with Gravity Compensation

REFERENCES

[1] *S. Kajita, F. Kanehiro, K. Kaneko, K. Fujiwara, K. Harada, K. Yokoi and H. Hirukawa*, "Biped Walking Pattern Generation by using Preview Control of Zero-Moment Point", IEEE International Conference on Robotics & Automation, pp. 1620-1626, 2003.

[2] *L. W. Lee*, "Biped Robot Gaiting Using Trajectory Planning and Robust PID Control System", master thesis, 2007.

[3] *J. W. Tseng,* "The Development of Biped Robot Gaiting Using Fuzzy Control System", master thesis, 2007.

[4] http://en.wikipedia.org/wiki/ASIMO

[5] http://www.bostondynamics.com/robot_petman.html

[6] http://www.takanishi.mech.waseda.ac.jp/top/research/wabian/previous_reserch/previous_research.htm

[7] http://www.takanishi.mech.waseda.ac.jp/top/research/wabian/index.htm

[8] *M. Vukobratović, D. Juričić*, "Zero-Moment Point- Thirty Five Years of Its Life", IEEE International Journal of Humanoid Robotics, pp.157~173, 2004.

[9] http://tw.myblog.yahoo.com/jw!XgzgP9.CBBTniZt5r7jKzA--/article?mid=2697

[10] *Alexander,* "Elastic Mechanisms in Animal Movement 1988: Cambridge

University Press".

[11] *McMahon,* Elastic Mechanisms in Animal Movement - Alexander, R.M. Nature, 1988. 336(6199): p. 530-530.

[12] *Blickhan,* The spring mass model for running and hopping. Journal of Biomechanics, 1989. 22(11-12): p. 1217-1227.

[13] *R. C. Luo, H. Y. Chang, H. H. Chang and Y. P. Yang,* "Walking Pattern Based on Simulated Annealing for Biped Robotics", 2011 IEEE World Congress on Intelligent Control and Automation, Taipei, R.O.C..

[14] *Q. Huang, K. Yokoi, S. Kajita, K. Kaneko, H. Arai, N. Koyachi and K. Tanie* "Planning Walking Patterns for a Biped Robot" *IEEE Transactions on Robotics and Automation,* vol. 17, NO. 3, pp. 280-289, 2001

[15] *R.C. Luo, H.Y. Chang ,and J.W. Chen,* "The development of fuzzy virtual spring-damper generator for reducing biped walking contact vibration", 2010 Advance Robotics and its Social Impacts, Seoul, Korea.

[16] Q. Li, A. Takanishi and I. Kato, "A Biped Walking Robot Having A ZMP Measurement System Using Universal Force-Moment Sensors" IEEE/RSJ International Workshop on Intelligent Robots and Systems lROS '91. Nov. 3-5, 1991, pp. 1568-1573, Osaka, Japan IEEE.

[17] *J. I. Yamaguchi, A. Takanishi, and I. Kato*, "Development of a Biped Walking

Robot Compensating for Three-Axis Moment by Trunk Motion", Proceedings of the 1993 IEEE/RSJ Intemational Conference on Intelligent Robots and Systems Yokohama, Japan July 26-30.1993, pp. 561-566.

[18] *J. I. Yamaguchi, E. Soga, S. Inoue and A. Takanishi,* "Development of a Bipedal Humanoid Robot Control Method of Whole Body Cooperative Dynamic Biped Walking" Proceedings of the 1999 EEE International Conference on Robotics & Automation Detroit, Michigan May 1999, pp. 368-374.

[19] *Q. Li, A. Takanishi, and I. Kato*, Learning Control of Compensative Trunk Motion for Biped Walking Robot based on ZMP Stability Criterion, Proceedings of the 1992 IEEE/RSJ International Conference on Intelligent Robots and Systems, Raleigh, NC July 7-10,1992, pp.597-603.

VITA

姓名：張宏毅

性別：男

生日：1987/09/22

籍貫：台灣 - 嘉義

學歷：

1. 民國 100 年 7 月　　國立台灣大學機械工程研究所畢業
2. 民國 98 年 6 月　　國立中正大學機械工程學系畢業

發表著作：

3. *R.C. Luo, IEEE, H.Y Chang ,and J.W Chen,* "The development of fuzzy virtual spring-damper generator for reducing biped walking contact vibration", 2010 Advance Robotics and its Social Impacts, Seoul, Korea.
4. *R. C. Luo, H. Y. Chang, H. H. Chang and Y. P. Yang,* "Walking Pattern Based on Simulated Annealing for Biped Robotics", 2011 IEEE World Congress on Intelligent Control and Automation, Taipei, R.O.C..

榮譽事項：

2010/10/22 智慧型機器人產品創意競賽-夢想實現組 榮獲 第三名